An augmented mixed finite element method for 3D linear elasticity problems[☆]

Gabriel N. Gatica [a,*], Antonio Márquez [b], Salim Meddahi [c]

[a] CI^{2}MA and Departamento de Ingeniería Matemática, Facultad de Ciencias Físicas y Matemáticas, Universidad de Concepción, Casilla 160-C, Concepción, Chile
[b] Departamento de Construcción e Ingeniería de Fabricación, Universidad de Oviedo, Oviedo, Espagne
[c] Departamento de Matemáticas, Facultad de Ciencias, Universidad de Oviedo, Calvo Sotelo s/n, Oviedo, Espagne

ARTICLE INFO

ABSTRACT

In this paper we introduce and analyze a new augmented mixed finite element method for linear elasticity problems in 3D. Our approach is an extension of a technique developed recently for plane elasticity, which is based on the introduction of consistent terms of Galerkin least-squares type. We consider non-homogeneous and homogeneous Dirichlet boundary conditions and prove that the resulting augmented variational formulations lead to strongly coercive bilinear forms. In this way, the associated Galerkin schemes become well posed for arbitrary choices of the corresponding finite element subspaces. In particular, Raviart–Thomas spaces of order 0 for the stress tensor, continuous piecewise linear elements for the displacement, and piecewise constants for the rotation can be utilized. Moreover, we show that in this case the number of unknowns behaves approximately as 9.5 times the number of elements (tetrahedrons) of the triangulation, which is cheaper, by a factor of 3, than the classical *PEERS* in 3D. Several numerical results illustrating the good performance of the augmented schemes are provided.

1. Introduction

The analysis of a new augmented mixed finite element method for plane linear elasticity with homogeneous Dirichlet boundary conditions was presented in [1]. The approach there is based on the introduction of the Galerkin least-squares type terms arising from the constitutive and equilibrium equations, and from the relation defining the rotation in terms of the displacement, all of them multiplied by suitably chosen stabilization parameters. In this way, the augmented formulation becomes strongly coercive, and hence arbitrary finite element subspaces can be considered to define the associated discrete scheme. In particular, Raviart–Thomas spaces of order 0 for the stress tensor, continuous piecewise linear elements for the displacement, and piecewise constants for the rotation, which are known to yield a non-feasible choice for the usual mixed formulation, constitute the lowest order susbspaces that can be used in the augmented method. Furthermore, if we assume uniform refinements, the total number of unknowns behaves in this case approximately as 5 times the number of triangles of each triangulation. This is certainly cheaper than employing the well-known *PEERS* (see [2]) in the usual non-augmented formulation, where the corresponding factor becomes 7.5.

Now, a residual based a posteriori error analysis yielding a reliable and efficient estimator for the augmented method from [1], is provided in [3], which confirms that this approach is also suitable for adaptive computations. It is worth

---

* Corresponding author.
E-mail addresses: ggatica@ing-mat.udec.cl (G.N. Gatica), amarquez@uniovi.es (A. Márquez), salim@orion.ciencias.uniovi.es (S. Meddahi).

mentioning that the analysis in [1,3] requires the application of the first Korn inequality (see, e.g. Theorem 10.1 in [4]), and therefore only homogeneous Dirichlet boundary conditions were considered there. Nevertheless, the corresponding extension to plane linear elasticity with non-homogeneous Dirichlet boundary conditions was performed recently in [5]. The introduction of an additional consistent term and the application of a slight modification of the classical Korn inequality are the main novelties of the analysis in [5].

According to the above, the purpose of this paper is to extend the results from [1,5] to 3D linear elasticity problems, while keeping the same advantages of the 2D case in the resulting augmented formulation. In particular, we observe that if we employ Raviart–Thomas spaces of order 0 for the stress tensor, continuous piecewise linear elements for the displacement, and piecewise constants for the rotation, then the total number of unknowns behaves approximately as 9.5 times the number of tetrahedrons of the triangulation. This factor increases to 12.5 when the 3D *PEERS* (see, e.g., Definition 3.1 in [6]) is used in the non-augmented formulation, which confirms that the augmented mixed finite element scheme is also cheaper than *PEERS* in 3D. The rest of this paper is organized as follows. In Section 2 we describe the 3D linear elasticity problem with non-homogeneous Dirichlet boundary conditions, and establish its dual-mixed variational formulation. In Section 3 we define the augmented dual-mixed variational formulation and show that it is well posed. The analysis here includes the application of a modified Korn inequality. As a consequence, the choice of some stabilization parameters depend on an unknown constant appearing in this inequality, whereas the rest of them are determined explicitly by the bounded Lamé constant. Then, in Section 4 we introduce the augmented mixed finite element scheme and show that the specific finite element subspace mentioned above does yield the announced factor 9.5. A priori error estimates and rates of convergence are also given here. In Section 5 we consider the case of homogeneous Dirichlet boundary conditions and simplify accordingly the analysis from Sections 3 and 4. In particular, we prove in this case that all the stabilization parameters can be computed explicitly. Next, several numerical results illustrating the good performance of the augmented scheme are reported in Section 6. Finally, a proof of the above-mentioned modified Korn inequality is given in the Appendix.

We end this section by introducing some notations to be used throughout the paper. For each Hilbert space U, we let U^3 and $U^{3\times 3}$ be, respectively, the space of vectors and square matrices of order 3 with entries in U. In addition, given $\boldsymbol{\tau} := (\tau_{ij})$, $\boldsymbol{\zeta} := (\zeta_{ij}) \in \mathbb{R}^{3\times 3}$, we define the transpose tensor $\boldsymbol{\tau}^{\mathrm{t}} := (\tau_{ji})$, the trace $\mathrm{tr}(\boldsymbol{\tau}) := \sum_{i=1}^{3} \tau_{ii}$, the tensor product $\boldsymbol{\tau} : \boldsymbol{\zeta} := \sum_{i,j=1}^{3} \tau_{ij} \zeta_{ij}$, and the deviator $\boldsymbol{\tau}^{\mathrm{d}} := \boldsymbol{\tau} - \frac{1}{3}\mathrm{tr}(\boldsymbol{\tau})\,\mathbf{I}$, where $\mathbf{I}$ is the identity matrix of $\mathbb{R}^{3\times 3}$. Also, in what follows we utilize the standard terminology for Sobolev spaces and norms, employ $\mathbf{0}$ to denote a generic null vector, and use C, with or without subscripts, bars, tildes or hats, to denote generic constants independent of the discretization parameters, which may take different values at different places.

2. The model problem

Let Ω be a simply connected domain in $\mathbb{R}^3$ with polyhedric boundary $\Gamma := \partial\Omega$. We are interested in determining the small displacement $\mathbf{u}$ and the stress tensor $\boldsymbol{\sigma}$ of an isotropic linear elastic material occupying the region Ω. In other words, given a volume force $\mathbf{f} \in [L^2(\Omega)]^3$ and a Dirichlet datum $\mathbf{g} \in [H^{1/2}(\Gamma)]^3$, we seek a symmetric tensor field $\boldsymbol{\sigma}$ and a vector field $\mathbf{u}$ such that

$$\mathbf{div}(\boldsymbol{\sigma}) = -\mathbf{f} \quad \text{in } \Omega, \qquad \mathbf{e}(\mathbf{u}) = \frac{1}{2}(\nabla\mathbf{u} + (\nabla\mathbf{u})^{\mathrm{t}}) \quad \text{in } \Omega,$$
$$\boldsymbol{\sigma} = \mathcal{C}\mathbf{e}(\mathbf{u}) \quad \text{in } \Omega, \quad \text{and} \quad \mathbf{u} = \mathbf{g} \quad \text{on } \Gamma. \tag{2.1}$$

Hereafter, **div** stands for the usual divergence operator div acting along each row of the tensor and $\mathbf{e}$ is the infinitesimal strain tensor. The first and second equations of (2.1) correspond, respectively, to the equilibrium of forces in Ω and the linear geometric compatibility in the solid between strains and displacements. The third equation is the constitutive Hooke's law given by

$$\mathcal{C}\boldsymbol{\zeta} := \lambda\,\mathrm{tr}(\boldsymbol{\zeta})\mathbf{I} + 2\mu\boldsymbol{\zeta} \quad \forall\,\boldsymbol{\zeta} \in [L^2(\Omega)]^3, \tag{2.2}$$

where $\lambda, \mu > 0$ are the Lamé elastic constants of the solid. Then, it is easy to see from (2.2) that the inverse of the elasticity operator $\mathcal{C}$ reduces to

$$\mathcal{C}^{-1}\boldsymbol{\zeta} := \frac{1}{2\mu}\boldsymbol{\zeta} - \frac{\lambda}{2\mu(3\lambda + 2\mu)}\mathrm{tr}(\boldsymbol{\zeta})\mathbf{I}. \tag{2.3}$$

We now follow the classical stress–displacement–rotation formulation (see [2,7]). In fact, imposing weakly the symmetry of $\boldsymbol{\sigma}$ through the introduction of the rotation $\boldsymbol{\gamma} := \frac{1}{2}(\nabla\mathbf{u} - (\nabla\mathbf{u})^{\mathrm{t}})$ as a further unknown, multiplying by test functions, and then integrating the equilibrium equation and the relation $\nabla\mathbf{u} - \boldsymbol{\gamma} = \mathbf{e}(\mathbf{u}) = \mathcal{C}^{-1}\boldsymbol{\sigma}$ (see (2.3)), we end up with the following dual-mixed variational formulation of (2.1)–(2.2): Find $(\boldsymbol{\sigma}, (\mathbf{u}, \boldsymbol{\gamma})) \in H \times Q$ such that

$$a(\boldsymbol{\sigma}, \boldsymbol{\tau}) + b(\boldsymbol{\tau}, (\mathbf{u}, \boldsymbol{\gamma})) = \langle \boldsymbol{\tau}\,\nu, \mathbf{g}\rangle \quad \forall\,\boldsymbol{\tau} \in H,$$
$$b(\boldsymbol{\sigma}, (\mathbf{v}, \boldsymbol{\eta})) = -\int_{\Omega} \mathbf{f} \cdot \mathbf{v} \quad \forall\,(\mathbf{v}, \boldsymbol{\eta}) \in Q, \tag{2.4}$$

where $\langle \cdot, \cdot \rangle$ stands for the duality pairing of $[H^{-1/2}(\Gamma)]^3$ and $[H^{1/2}(\Gamma)]^3$ with respect to the $[L^2(\Gamma)]^3$-inner product,

$$H = H(\mathbf{div}; \Omega) := \left\{ \boldsymbol{\tau} \in [L^2(\Omega)]^{3\times 3} : \mathbf{div}(\boldsymbol{\tau}) \in [L^2(\Omega)]^3 \right\},$$

$$Q := [L^2(\Omega)]^3 \times [L^2(\Omega)]^{3\times 3}_{\mathrm{asym}}, \quad [L^2(\Omega)]^{3\times 3}_{\mathrm{asym}} := \left\{ \boldsymbol{\eta} \in [L^2(\Omega)]^{3\times 3} : \quad \boldsymbol{\eta} + \boldsymbol{\eta}^{\mathrm{t}} = 0 \right\},$$

and the bilinear forms $a : H \times H \to \mathbb{R}$ and $b : H \times Q \to \mathbb{R}$ are defined by

$$a(\boldsymbol{\zeta}, \boldsymbol{\tau}) := \int_{\Omega} \mathcal{C}^{-1} \boldsymbol{\zeta} : \boldsymbol{\tau} = \frac{1}{2\,\mu} \int_{\Omega} \boldsymbol{\zeta} : \boldsymbol{\tau} - \frac{\lambda}{2\,\mu\,(3\,\lambda + 2\,\mu)} \int_{\Omega} \mathrm{tr}(\boldsymbol{\zeta})\,\mathrm{tr}(\boldsymbol{\tau}) \tag{2.5}$$

and

$$b(\boldsymbol{\tau}, (\mathbf{v}, \boldsymbol{\eta})) := \int_{\Omega} \mathbf{v} \cdot \mathbf{div}(\boldsymbol{\tau}) + \int_{\Omega} \boldsymbol{\eta} : \boldsymbol{\tau}, \tag{2.6}$$

for all $\boldsymbol{\zeta}, \boldsymbol{\tau} \in H$ and for all $(\mathbf{v}, \boldsymbol{\eta}) \in Q$. It follows easily from (2.5) and (2.6) that for any $(\boldsymbol{\tau}, (\mathbf{v}, \boldsymbol{\eta}), c) \in [L^2(\Omega)]^{3\times 3} \times Q \times \mathbb{R}$ there holds

$$a(c\,\mathbf{I}, \boldsymbol{\tau}) = \frac{c}{(3\,\lambda + 2\,\mu)} \int_{\Omega} \mathrm{tr}(\boldsymbol{\tau}) \quad \text{and} \quad b(c\,\mathbf{I}, (\mathbf{v}, \boldsymbol{\eta})) = 0. \tag{2.7}$$

Also, it is important to observe that a can be rewritten as

$$a(\boldsymbol{\zeta}, \boldsymbol{\tau}) = \frac{1}{2\,\mu} \int_{\Omega} \boldsymbol{\zeta}^{\mathrm{d}} : \boldsymbol{\tau}^{\mathrm{d}} + \frac{1}{3\,(3\,\lambda + 2\,\mu)} \int_{\Omega} \mathrm{tr}(\boldsymbol{\zeta})\,\mathrm{tr}(\boldsymbol{\tau}), \tag{2.8}$$

which implies that

$$a(\boldsymbol{\tau}, \boldsymbol{\tau}) \geq \frac{1}{2\mu} \|\boldsymbol{\tau}^{\mathrm{d}}\|^2_{[L^2(\Omega)]^{3\times 3}} \qquad \forall \boldsymbol{\tau} \in [L^2(\Omega)]^{3\times 3}. \tag{2.9}$$

We now define $H_0 := \left\{ \boldsymbol{\tau} \in H : \int_{\Omega} \mathrm{tr}(\boldsymbol{\tau}) = 0 \right\}$ and note that $H = H_0 \oplus \mathbb{R}\,\mathbf{I}$, that is for any $\boldsymbol{\tau} \in H$ there exist unique $\boldsymbol{\tau}_0 \in H_0$ and $d := \frac{1}{3|\Omega|} \int_{\Omega} \mathrm{tr}(\boldsymbol{\tau}) \in \mathbb{R}$ such that $\boldsymbol{\tau} = \boldsymbol{\tau}_0 + d\,\mathbf{I}$. In particular, we obtain from (2.1) and (2.2) that

$$\mathrm{tr}(\boldsymbol{\sigma}) = (3\,\lambda + 2\,\mu)\,\mathrm{tr}\,\mathbf{e}(\mathbf{u}) = (3\,\lambda + 2\,\mu)\,\mathrm{div}(\mathbf{u}),$$

which yields $\boldsymbol{\sigma} = \boldsymbol{\sigma}_0 + c\,\mathbf{I}$, with $\boldsymbol{\sigma}_0 \in H_0$ and the constant c given explicitly by

$$c := \frac{1}{3\,|\Omega|} \int_{\Omega} \mathrm{tr}(\boldsymbol{\sigma}) = \frac{(3\,\lambda + 2\,\mu)}{3\,|\Omega|} \int_{\Gamma} \mathbf{g} \cdot \boldsymbol{v}. \tag{2.10}$$

In this way, replacing $\boldsymbol{\sigma}$ by the expression $\boldsymbol{\sigma}_0 + c\,\mathbf{I}$ in (2.4), applying the identities given in (2.7), and denoting from now on the remaining unknown $\boldsymbol{\sigma}_0 \in H_0$ simply by $\boldsymbol{\sigma}$, we find that the dual-mixed variational formulation of (2.1) reduces to: Find $(\boldsymbol{\sigma}, (\mathbf{u}, \boldsymbol{\gamma})) \in H_0 \times Q$ such that

$$a(\boldsymbol{\sigma}, \boldsymbol{\tau}) + b(\boldsymbol{\tau}, (\mathbf{u}, \boldsymbol{\gamma})) = \langle \boldsymbol{\tau}\,\boldsymbol{v}, \mathbf{g} \rangle \quad \forall \boldsymbol{\tau} \in H_0,$$
$$b(\boldsymbol{\sigma}, (\mathbf{v}, \boldsymbol{\eta})) = -\int_{\Omega} \mathbf{f} \cdot \mathbf{v} \quad \forall (\mathbf{v}, \boldsymbol{\eta}) \in Q. \tag{2.11}$$

Furthermore, according to the new meaning of $\boldsymbol{\sigma}$, we deduce from (2.10) and (2.3) that the constitutive equation in (2.1) now becomes

$$\mathbf{e}(\mathbf{u}) - \mathcal{C}^{-1}(\boldsymbol{\sigma}) = \left\{ \frac{1}{3\,|\Omega|} \int_{\Gamma} \mathbf{g} \cdot \boldsymbol{v} \right\} \mathbf{I} \quad \text{in } \Omega, \tag{2.12}$$

whereas the equilibrium equation remains the same, that is $\mathbf{div}\,(\boldsymbol{\sigma}) = -\mathbf{f}$ in Ω.

We end this section by remarking that the well-posedness of (2.11), whose proof follows from the classical Babuška–Brezzi theory (see, e.g. [8]), yields a continuous dependence result independently of the Lamé constant λ. We refer to [2] or [9] for details (see also Section 2.1 in [1]). We only recall here for later use the following result concerning H_0, which is fundamental in that proof.

Lemma 2.1. *There exists $c_1 > 0$, depending only on Ω, such that*

$$c_1 \|\boldsymbol{\tau}\|^2_{[L^2(\Omega)]^{3\times 3}} \leq \|\boldsymbol{\tau}^{\mathrm{d}}\|^2_{[L^2(\Omega)]^{3\times 3}} + \|\mathbf{div}(\boldsymbol{\tau})\|^2_{[L^2(\Omega)]^3} \quad \forall \boldsymbol{\tau} \in H_0. \tag{2.13}$$

Proof. It is a analogous to the corresponding proof for the 2D case (see Lemma 3.1 in [10] or Proposition 3.1 of Chapter IV in [8]). □

3. The augmented dual-mixed variational formulation

In this section we follow the original approach from [1] and enrich the dual-mixed variational formulation (2.11) with Galerkin least-squares type terms arising from the constitutive and equilibrium equations, and from the relation defining the rotation as a function of the displacement. Recall that the constitutive equation is given now by (2.12). Furthermore, in order to deal with the non-homogeneous Dirichlet boundary condition, we proceed as in [5] and introduce a consistent boundary term. In other words, we first subtract the second from the first equation of (2.11) and then add

$$\kappa_1 \int_{\Omega} \left(\mathbf{e}(\mathbf{u}) - \mathcal{C}^{-1} \boldsymbol{\sigma} \right) : \left(\mathbf{e}(\mathbf{v}) + \mathcal{C}^{-1} \boldsymbol{\tau} \right) = \kappa_1 \left\{ \frac{1}{3 \, |\Omega|} \int_{\Gamma} \mathbf{g} \cdot \boldsymbol{\nu} \right\} \int_{\Omega} \mathbf{I} : \left(\mathbf{e}(\mathbf{v}) + \mathcal{C}^{-1} \boldsymbol{\tau} \right),$$

$$\kappa_2 \int_{\Omega} \mathbf{div}(\boldsymbol{\sigma}) \cdot \mathbf{div}(\boldsymbol{\tau}) = -\kappa_2 \int_{\Omega} \mathbf{f} \cdot \mathbf{div}(\boldsymbol{\tau}),$$

$$\kappa_3 \int_{\Omega} \left(\boldsymbol{\gamma} - \frac{1}{2}(\nabla \mathbf{u} - (\nabla \mathbf{u})^{\mathrm{t}}) \right) : \left(\boldsymbol{\eta} + \frac{1}{2}(\nabla \mathbf{v} - (\nabla \mathbf{v})^{\mathrm{t}}) \right) = 0,$$

and

$$\kappa_4 \int_{\Gamma} \mathbf{u} \cdot \mathbf{v} = \kappa_4 \int_{\Gamma} \mathbf{g} \cdot \mathbf{v},$$

for all $(\boldsymbol{\tau}, \mathbf{v}, \boldsymbol{\eta}) \in H_0 \times [H^1(\Omega)]^3 \times [L^2(\Omega)]^{3 \times 3}_{\mathrm{asym}}$, where $(\kappa_1, \kappa_2, \kappa_3, \kappa_4)$ is a vector of positive constants, also named stabilization parameters, to be specified later on, independently of the Lamé constant λ. It is important to observe here that the above terms require now the displacement $\mathbf{u}$ to live in $[H^1(\Omega)]^3$. In addition, it follows easily from (2.3) that

$$\mathrm{tr}\left(\mathcal{C}^{-1} \boldsymbol{\tau} \right) = \frac{1}{(3 \, \lambda + 2 \, \mu)} \, \mathrm{tr}(\boldsymbol{\tau}) \quad \forall \, \boldsymbol{\tau} \in H,$$

and hence for each $\boldsymbol{\tau} \in H_0$ there holds

$$\int_{\Omega} \mathbf{I} : \left(\mathbf{e}(\mathbf{v}) + \mathcal{C}^{-1} \boldsymbol{\tau} \right) = \int_{\Omega} \mathrm{tr}\left(\mathbf{e}(\mathbf{v}) + \mathcal{C}^{-1} \boldsymbol{\tau} \right) = \int_{\Omega} \mathrm{div}(\mathbf{v}) = \int_{\Gamma} \mathbf{v} \cdot \boldsymbol{\nu}.$$

In this way, instead of (2.11) we propose the following augmented dual-mixed variational formulation: Find $(\boldsymbol{\sigma}, \mathbf{u}, \boldsymbol{\gamma}) \in \mathbf{H}_0 := H_0 \times [H^1(\Omega)]^3 \times [L^2(\Omega)]^{3 \times 3}_{\mathrm{asym}}$ such that

$$A((\boldsymbol{\sigma}, \mathbf{u}, \boldsymbol{\gamma}), (\boldsymbol{\tau}, \mathbf{v}, \boldsymbol{\eta})) = F(\boldsymbol{\tau}, \mathbf{v}, \boldsymbol{\eta}) \quad \forall \, (\boldsymbol{\tau}, \mathbf{v}, \boldsymbol{\eta}) \in \mathbf{H}_0, \tag{3.1}$$

where the bilinear form $A : \mathbf{H}_0 \times \mathbf{H}_0 \to \mathbb{R}$ and the functional $F : \mathbf{H}_0 \to \mathbb{R}$ are defined by

$$A((\boldsymbol{\sigma}, \mathbf{u}, \boldsymbol{\gamma}), (\boldsymbol{\tau}, \mathbf{v}, \boldsymbol{\eta})) := \int_{\Omega} \mathcal{C}^{-1} \boldsymbol{\sigma} : \boldsymbol{\tau} + \int_{\Omega} \mathbf{u} \cdot \mathbf{div}(\boldsymbol{\tau}) + \int_{\Omega} \boldsymbol{\gamma} : \boldsymbol{\tau} - \int_{\Omega} \mathbf{v} \cdot \mathbf{div}(\boldsymbol{\sigma}) - \int_{\Omega} \boldsymbol{\eta} : \boldsymbol{\sigma}$$

$$+ \kappa_1 \int_{\Omega} \left(\mathbf{e}(\mathbf{u}) - \mathcal{C}^{-1} \boldsymbol{\sigma} \right) : \left(\mathbf{e}(\mathbf{v}) + \mathcal{C}^{-1} \boldsymbol{\tau} \right) + \kappa_2 \int_{\Omega} \mathbf{div}(\boldsymbol{\sigma}) \cdot \mathbf{div}(\boldsymbol{\tau})$$

$$+ \kappa_3 \int_{\Omega} \left(\boldsymbol{\gamma} - \frac{1}{2}(\nabla \mathbf{u} - (\nabla \mathbf{u})^{\mathrm{t}}) \right) : \left(\boldsymbol{\eta} + \frac{1}{2}(\nabla \mathbf{v} - (\nabla \mathbf{v})^{\mathrm{t}}) \right) + \kappa_4 \int_{\Gamma} \mathbf{u} \cdot \mathbf{v}, \tag{3.2}$$

and

$$F(\boldsymbol{\tau}, \mathbf{v}, \boldsymbol{\eta}) := \int_{\Omega} \mathbf{f} \cdot (\mathbf{v} - \kappa_2 \, \mathbf{div}(\boldsymbol{\tau})) + \langle \boldsymbol{\tau} \, \boldsymbol{\nu}, \mathbf{g} \rangle + \kappa_4 \int_{\Gamma} \mathbf{g} \cdot \mathbf{v} + \kappa_1 \, c_{\mathbf{g}} \int_{\Gamma} \mathbf{v} \cdot \boldsymbol{\nu}, \tag{3.3}$$

with

$$c_{\mathbf{g}} := \left\{ \frac{1}{3 \, |\Omega|} \int_{\Gamma} \mathbf{g} \cdot \boldsymbol{\nu} \right\}.$$

In what follows we proceed as in [1,5] and derive sufficient conditions on the parameters κ_1, κ_2, κ_3, and κ_4, ensuring that A becomes strongly coercive and bounded in $\mathbf{H}_0$, with constants independent of λ, with respect to the norm $\| \cdot \|_{\mathbf{H}_0}$ defined by

$$\|(\boldsymbol{\tau}, \mathbf{v}, \boldsymbol{\eta})\|_{\mathbf{H}_0} := \left\{ \|\boldsymbol{\tau}\|^2_{H(\mathbf{div}; \, \Omega)} + \|\mathbf{v}\|^2_{[H^1(\Omega)]^3} + \|\boldsymbol{\eta}\|^2_{[L^2(\Omega)]^{3 \times 3}} \right\}^{1/2} \quad \forall \, (\boldsymbol{\tau}, \mathbf{v}, \boldsymbol{\eta}) \in \mathbf{H}_0. \tag{3.4}$$

For this purpose, we need a slight modification of the classical Korn inequality, which establishes the existence of a constant $\kappa_0 > 0$ such that

$$\|\mathbf{e}(\mathbf{v})\|^2_{[L^2(\Omega)]^{3 \times 3}} + \|\mathbf{v}\|^2_{[L^2(\Gamma)]^3} \geq \kappa_0 \|\mathbf{v}\|^2_{[H^1(\Omega)]^3} \quad \forall \, \mathbf{v} \in [H^1(\Omega)]^3. \tag{3.5}$$

The proof of (3.5) follows similar compactness arguments to those employed in the demonstration of the first Korn inequality (see, e.g. Theorem 9.2.16 in [11] or Theorem 2.2 in [12]). For the sake of completeness, in the Appendix of this paper we provide a proof of (3.5) that makes use of the Peetre–Tartar Lemma (cf. Theorem 2.1 in Chapter I of [13]).

Now, let us first notice that

$$\int_{\Omega} \left(\mathbf{e}(\mathbf{v}) - \mathcal{C}^{-1} \boldsymbol{\tau} \right) : \left(\mathbf{e}(\mathbf{v}) + \mathcal{C}^{-1} \boldsymbol{\tau} \right) = \|\mathbf{e}(\mathbf{v})\|^2_{[L^2(\Omega)]^{3\times 3}} - \|\mathcal{C}^{-1}\boldsymbol{\tau}\|^2_{[L^2(\Omega)]^{3\times 3}},$$

and

$$\int_{\Omega} \left(\boldsymbol{\eta} - \frac{1}{2}(\nabla\mathbf{v} - (\nabla\mathbf{v})^{\mathrm{t}}) \right) : \left(\boldsymbol{\eta} + \frac{1}{2}(\nabla\mathbf{v} - (\nabla\mathbf{v})^{\mathrm{t}}) \right) = \|\boldsymbol{\eta}\|^2_{[L^2(\Omega)]^{3\times 3}} + \|\mathbf{e}(\mathbf{v})\|^2_{[L^2(\Omega)]^{3\times 3}} - |\mathbf{v}|^2_{[H^1(\Omega)]^3}.$$

Next, using (2.5) and the inverse relation (2.3), we find that

$$\int_{\Omega} \mathcal{C}^{-1}\boldsymbol{\tau} : \boldsymbol{\tau} - \kappa_1 \|\mathcal{C}^{-1}\boldsymbol{\tau}\|^2_{[L^2(\Omega)]^{3\times 3}} = \frac{1}{2\mu} \left\{ \|\boldsymbol{\tau}\|^2_{[L^2(\Omega)]^{3\times 3}} - \frac{\lambda}{(3\lambda + 2\mu)} \int_{\Omega} \mathrm{tr}^2(\boldsymbol{\tau}) \right\}$$

$$- \frac{\kappa_1}{4\mu^2} \left\{ \|\boldsymbol{\tau}\|^2_{[L^2(\Omega)]^{3\times 3}} - 2\left(\frac{\lambda}{3\lambda + 2\mu} \right) \int_{\Omega} \mathrm{tr}^2(\boldsymbol{\tau}) + 3 \left(\frac{\lambda}{3\lambda + 2\mu} \right)^2 \int_{\Omega} \mathrm{tr}^2(\boldsymbol{\tau}) \right\}$$

$$= \frac{1}{2\mu} \left(1 - \frac{\kappa_1}{2\mu} \right) \|\boldsymbol{\tau}^{\mathrm{d}}\|^2_{[L^2(\Omega)]^{3\times 3}} + \frac{1}{3(3\lambda + 2\mu)} \left(1 - \frac{\kappa_1}{(3\lambda + 2\mu)} \right) \int_{\Omega} \mathrm{tr}^2(\boldsymbol{\tau}).$$

In this way, according to the definition of A (cf. (3.2)) and the above identities, we can write

$$A((\boldsymbol{\tau}, \mathbf{v}, \boldsymbol{\eta}), (\boldsymbol{\tau}, \mathbf{v}, \boldsymbol{\eta})) = \frac{1}{2\mu} \left(1 - \frac{\kappa_1}{2\mu} \right) \|\boldsymbol{\tau}^{\mathrm{d}}\|^2_{[L^2(\Omega)]^{3\times 3}} + \frac{1}{3(3\lambda + 2\mu)} \left(1 - \frac{\kappa_1}{(3\lambda + 2\mu)} \right) \int_{\Omega} \mathrm{tr}^2(\boldsymbol{\tau})$$

$$+ \kappa_2 \|\mathbf{div}(\boldsymbol{\tau})\|^2_{[L^2(\Omega)]^3} + (\kappa_1 + \kappa_3) \|\mathbf{e}(\mathbf{v})\|^2_{[L^2(\Omega)]^{3\times 3}} - \kappa_3 |\mathbf{v}|^2_{[H^1(\Omega)]^3}$$

$$+ \kappa_4 \|\mathbf{v}\|^2_{[L^2(\Gamma)]^3} + \kappa_3 \|\boldsymbol{\eta}\|^2_{[L^2(\Omega)]^{3\times 3}} \quad \forall (\boldsymbol{\tau}, \mathbf{v}, \boldsymbol{\eta}) \in \mathbf{H}_0. \tag{3.6}$$

Hence, choosing the parameter κ_1 so that $0 < \kappa_1 < 2\mu$, which guarantees that $1 - \frac{\kappa_1}{2\mu} > 0$ and $1 - \frac{\kappa_1}{(3\lambda + 2\mu)} > 0$, and applying the estimates (2.13) (cf. Lemma 2.1) and (3.5), we deduce that

$$A((\boldsymbol{\tau}, \mathbf{v}, \boldsymbol{\eta}), (\boldsymbol{\tau}, \mathbf{v}, \boldsymbol{\eta})) \geq \alpha_2 \|\boldsymbol{\tau}\|^2_{H(\mathbf{div};\, \Omega)} + (\alpha_3\kappa_0 - \kappa_3) \|\mathbf{v}\|^2_{[H^1(\Omega)]^3} + \kappa_3 \|\boldsymbol{\eta}\|^2_{[L^2(\Omega)]^{3\times 3}} \tag{3.7}$$

for all $(\boldsymbol{\tau}, \mathbf{v}, \boldsymbol{\eta}) \in \mathbf{H}_0$, where

$$\alpha_2 := \min\left\{\alpha_1 c_1, \frac{\kappa_2}{2}\right\}, \qquad \alpha_1 := \min\left\{\frac{1}{2\mu}\left(1 - \frac{\kappa_1}{2\mu}\right), \frac{\kappa_2}{2}\right\}, \quad \text{and} \quad \alpha_3 := \min\{\kappa_1 + \kappa_3, \kappa_4\}.$$

We remark here that the introduction of the equation $\kappa_4 \int_{\Gamma} \mathbf{u} \cdot \mathbf{v} = \kappa_4 \int_{\Gamma} \mathbf{g} \cdot \mathbf{v} \quad \forall \mathbf{v} \in [H^1(\Omega)]^3$ in the augmented formulation (3.1), allows us to employ the inequality (3.5) in (3.6), which yields the term $\|\mathbf{v}\|^2_{[H^1(\Omega)]^3}$ in the estimate (3.7).

Next, we note that the only restriction on the parameters κ_2 and κ_4 is that both be positive. In particular, following [1,5], we can take $\kappa_2 = \frac{1}{\mu}\left(1 - \frac{\kappa_1}{2\mu}\right)$, whence $\alpha_1 = \frac{\kappa_2}{2}$ and $\alpha_2 = \frac{\kappa_2}{2}\min\{c_1, 1\}$. Also, we take for simplicity $\kappa_4 \geq \kappa_1 + \kappa_3$ so that α_3 becomes $\kappa_1 + \kappa_3$ and, in this way, the choice of κ_3 is determined by the value of κ_0. More precisely, if $\kappa_0 \geq 1$ it suffices to take any $\kappa_3 > 0$, whereas if $\kappa_0 < 1$ we choose κ_3 so that $0 < \kappa_3 < \left(\frac{\kappa_0}{1-\kappa_0}\right)\kappa_1$.

On the other hand, it is easy to see that A is bounded with a constant depending only on μ and the parameters $\kappa_1, \kappa_2, \kappa_3$, and κ_4.

We have thus shown the following result, which is the 3D analogue of Theorem 3.3 in [5].

Theorem 3.1. *Assume that $(\kappa_1, \kappa_2, \kappa_3, \kappa_4)$ is independent of λ and such that $0 < \kappa_1 < 2\mu$, $0 < \kappa_2$, $0 < \kappa_3 < \left(\frac{\kappa_0}{1-\kappa_0}\right)\kappa_1$ (if $\kappa_0 < 1$) or $\kappa_3 > 0$ (if $\kappa_0 \geq 1$), and $\kappa_4 \geq \kappa_1 + \kappa_3$. Then, there exist positive constants M, α, independent of λ, such that*

$$|A((\boldsymbol{\sigma}, \mathbf{u}, \boldsymbol{\gamma}), (\boldsymbol{\tau}, \mathbf{v}, \boldsymbol{\eta}))| \leq M \|(\boldsymbol{\sigma}, \mathbf{u}, \boldsymbol{\gamma})\|_{\mathbf{H}_0} \|(\boldsymbol{\tau}, \mathbf{v}, \boldsymbol{\eta})\|_{\mathbf{H}_0},$$

and

$$A((\boldsymbol{\tau}, \mathbf{v}, \boldsymbol{\eta}), (\boldsymbol{\tau}, \mathbf{v}, \boldsymbol{\eta})) \geq \alpha \|(\boldsymbol{\tau}, \mathbf{v}, \boldsymbol{\eta})\|^2_{\mathbf{H}_0}$$

for all $(\boldsymbol{\sigma}, \mathbf{u}, \boldsymbol{\gamma})$, $(\boldsymbol{\tau}, \mathbf{v}, \boldsymbol{\eta}) \in \mathbf{H}_0$. In particular, taking $\kappa_1 = C_1\mu$, with any $C_1 \in\,]0, 2[$, $\kappa_2 = \frac{1}{\mu}\left(1 - \frac{\kappa_1}{2\mu}\right)$, $\kappa_3 = C_3\kappa_1$, with any $C_3 \in\,]0, \frac{\kappa_0}{1-\kappa_0}[$ if $\kappa_0 < 1$, or $\kappa_3 = \kappa_1$ if $\kappa_0 \geq 1$, and $\kappa_4 = \kappa_1 + \kappa_3$, yields M and α depending only on μ, $\frac{1}{\mu}$, κ_0, and c_1.

We observe here, as announced in Section 1, that the stabilization parameters κ_3 and κ_4 depend on the unknown constant κ_0, whereas κ_1 and κ_2 are determined explicitly by the Lamé constant μ.

On the other hand, it is clear that the linear functional F (see (3.3)) is bounded independently of λ. Hence, the well-posedness of (3.1) follows as a simple consequence of Theorem 3.1 and the well-known Lax–Milgram Lemma.

Theorem 3.2. *Assume the same hypotheses of Theorem 3.1. Then the augmented variational formulation (3.1) has a unique solution $(\boldsymbol{\sigma}, \mathbf{u}, \boldsymbol{\gamma}) \in \mathbf{H}_0$, and there exists a positive constant C, depending only on μ, c_1, κ_0, κ_1, κ_2, and κ_4, such that*

$$\|(\boldsymbol{\sigma}, \mathbf{u}, \boldsymbol{\gamma})\|_{\mathbf{H}_0} \leq \frac{1}{\alpha} \|F\| \leq C \left\{ \|\mathbf{f}\|_{[L^2(\Omega)]^3} + \|\mathbf{g}\|_{[H^{1/2}(\Gamma)]^3} \right\}.$$

4. The augmented mixed finite element method

Given an arbitrary finite element subspace $\mathbf{H}_{0,h} \subseteq \mathbf{H}_0$, the Galerkin scheme associated with (3.1) reads: Find $(\boldsymbol{\sigma}_h, \mathbf{u}_h, \boldsymbol{\gamma}_h) \in \mathbf{H}_{0,h}$ such that

$$A((\boldsymbol{\sigma}_h, \mathbf{u}_h, \boldsymbol{\gamma}_h), (\boldsymbol{\tau}_h, \mathbf{v}_h, \boldsymbol{\eta}_h)) = F(\boldsymbol{\tau}_h, \mathbf{v}_h, \boldsymbol{\eta}_h) \quad \forall (\boldsymbol{\tau}_h, \mathbf{v}_h, \boldsymbol{\eta}_h) \in \mathbf{H}_{0,h}, \tag{4.1}$$

where A and F are defined by (3.2) and (3.3), respectively. In what follows we assume that (3.1) and (4.1) are defined with the same parameters κ_1, κ_2, κ_3, and κ_4 satisfying the assumptions of Theorem 3.1. Since A is bounded and strongly coercive on the whole space $\mathbf{H}_0$ (cf. Theorem 3.1), (4.1) is uniquely solvable. Moreover, there exist positive constants C, $\tilde{C}$, independent of λ and h, such that

$$\|(\boldsymbol{\sigma}_h, \mathbf{u}_h, \boldsymbol{\gamma}_h)\|_{\mathbf{H}_0} \leq C \sup_{\substack{(\boldsymbol{\tau}_h, \mathbf{v}_h, \boldsymbol{\eta}_h) \in \mathbf{H}_{0,h} \\ (\boldsymbol{\tau}_h, \mathbf{v}_h, \boldsymbol{\eta}_h) \neq 0}} \frac{|F(\boldsymbol{\tau}_h, \mathbf{v}_h, \boldsymbol{\eta}_h)|}{\|(\boldsymbol{\tau}_h, \mathbf{v}_h, \boldsymbol{\eta}_h)\|_{\mathbf{H}_0}} \leq C \left\{ \|\mathbf{f}\|_{[L^2(\Omega)]^3} + \|\mathbf{g}\|_{[H^{1/2}(\Gamma)]^3} \right\}$$

and

$$\|(\boldsymbol{\sigma}, \mathbf{u}, \boldsymbol{\gamma}) - (\boldsymbol{\sigma}_h, \mathbf{u}_h, \boldsymbol{\gamma}_h)\|_{\mathbf{H}_0} \leq \tilde{C} \inf_{(\boldsymbol{\tau}_h, \mathbf{v}_h, \boldsymbol{\eta}_h) \in \mathbf{H}_{0,h}} \|(\boldsymbol{\sigma}, \mathbf{u}, \boldsymbol{\gamma}) - (\boldsymbol{\tau}_h, \mathbf{v}_h, \boldsymbol{\eta}_h)\|_{\mathbf{H}_0}. \tag{4.2}$$

In order to define an explicit finite element subspace $\mathbf{H}_{0,h}$ of $\mathbf{H}_0$, we now let $\{\mathcal{T}_h\}_{h>0}$ be a regular family of triangulations of the polyhedric domain $\bar{\Omega}$ by tetrahedrons T of diameter h_T such that $h := \max\{h_T : T \in \mathcal{T}_h\}$. Given a non-negative integer k and $T \in \mathcal{T}_h$, $\mathbb{P}_k(T)$ stands for the space of polynomials in three variables defined in T of degree $\leq k$. In addition, for each $T \in \mathcal{T}_h$ we let $\mathbb{RT}_0(T)$ be the local Raviart–Thomas space of order 0, that is

$$\mathbb{RT}_0(T) := \text{span} \left\{ \begin{pmatrix} 1 \\ 0 \\ 0 \end{pmatrix}, \begin{pmatrix} 0 \\ 1 \\ 0 \end{pmatrix}, \begin{pmatrix} 0 \\ 0 \\ 1 \end{pmatrix}, \begin{pmatrix} x_1 \\ x_2 \\ x_3 \end{pmatrix} \right\} \subseteq [\mathbb{P}_1(T)]^3.$$

Then, we define

$$H_h^{\boldsymbol{\sigma}} := \{\boldsymbol{\tau}_h \in H(\mathbf{div}; \Omega) : \boldsymbol{\tau}_{h,i}|_T \in \mathbb{RT}_0(T) \, \forall i \in \{1, 2, 3\}, \, \forall T \in \mathcal{T}_h\}, \tag{4.3}$$

where $\boldsymbol{\tau}_{h,i}$ denotes the ith row of $\boldsymbol{\tau}_h$,

$$H_{0,h}^{\boldsymbol{\sigma}} := \left\{ \boldsymbol{\tau}_h \in H_h^{\boldsymbol{\sigma}} : \int_{\Omega} \text{tr}(\boldsymbol{\tau}_h) = 0 \right\}, \tag{4.4}$$

$$H_h^{\mathbf{u}} := \{\mathbf{v}_h \in [C(\bar{\Omega})]^3 : \mathbf{v}_h|_T \in [\mathbb{P}_1(T)]^3 \, \forall T \in \mathcal{T}_h\}, \tag{4.5}$$

$$H_h^{\boldsymbol{\gamma}} := \{\boldsymbol{\eta}_h \in [L^2(\Omega)]_{\text{asym}}^{3\times 3} : \boldsymbol{\eta}_h|_T \in [\mathbb{P}_0(T)]^{3\times 3} \, \forall T \in \mathcal{T}_h\}, \tag{4.6}$$

and

$$\mathbf{H}_{0,h} := H_{0,h}^{\boldsymbol{\sigma}} \times H_h^{\mathbf{u}} \times H_h^{\boldsymbol{\gamma}}. \tag{4.7}$$

It is well known that $\mathbf{H}_{0,h}$ is the finite element subspace of $\mathbf{H}_0 := H_0 \times [H^1(\Omega)]^3 \times [L^2(\Omega)]_{\text{asym}}^{3\times 3}$ of lowest order. Moreover, we claim that the number of degrees of freedom defining $\mathbf{H}_{0,h}$ behaves approximately as 9.5 times the total number of tetrahedrons of $\mathcal{T}_h$. In fact, let us assume for simplicity that the triangulation is obtained by refining cubes, as illustrated in Fig. 4.1 below. We see there that each cube is subdivided into the following 6 tetrahedrons (defined in terms of the corresponding vertices): ABDF, ADEF, EDFH, BCDF, CDFG, and DFGH. In addition, we observe that each vertex belongs to either 2 or 6 tetrahedrons in the cube, as indicated by the number between parentheses. Then, repeating this subdivision procedure in all the cubes defining the triangulation, as illustrated in Fig. 4.2 below where we display separately the four cubes sharing a common edge GC, we deduce that each interior vertex of the triangulation $\mathcal{T}_h$ belongs to 24 tetrahedrons. In fact, it is clear from this figure that the vertices G and C each belong to 12 tetrahedrons lying in the region delimited by those 4 cubes. However, if we assume that G and C are interior vertices of $\mathcal{T}_h$, then there must be another 4 cubes above G and another 4 cubes below C, thus making the total of 24 tetrahedrons for each one of them. According to this, the degrees of freedom defining $H_h^{\mathbf{u}}$ are given, approximately, by:

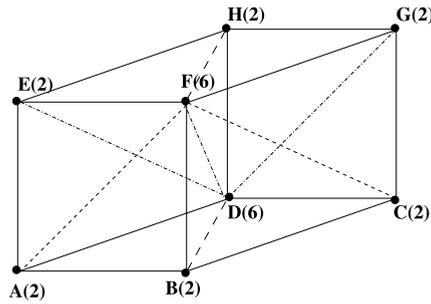$$\left(\frac{3 \times 4}{24} \right) \times m = 0.5 \times m,$$

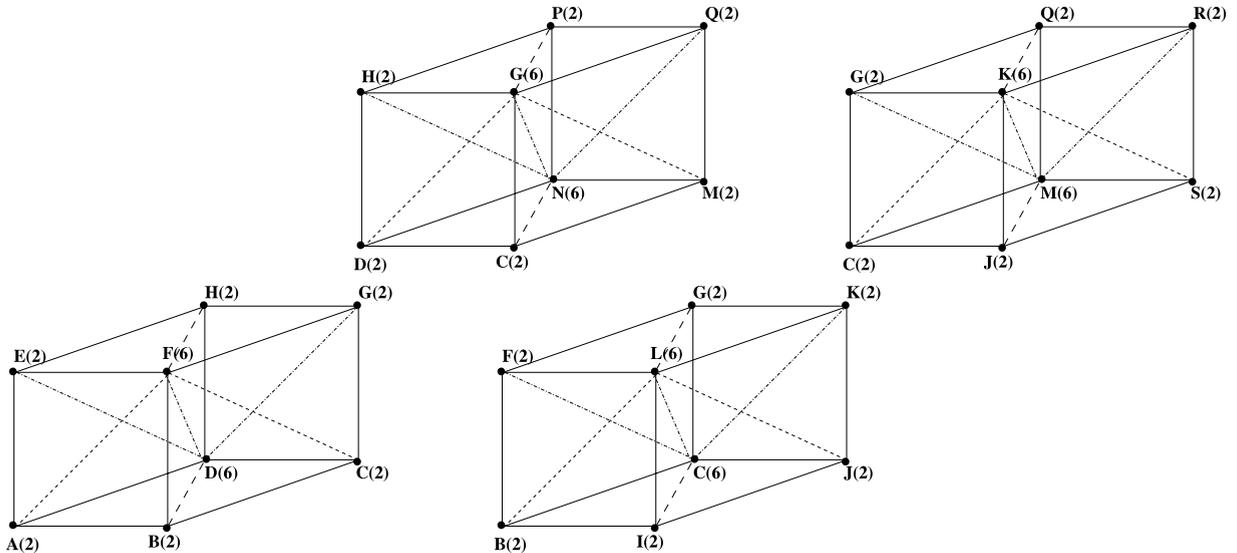**Fig. 4.1.** Subdivision of a cube into 6 tetrahedrons.

Fig. 4.2. Four cubes sharing the common edge GC.

where m is the total number of tetrahedrons of $\mathcal{T}_h$. Here, the expression "*approximately*" means that we are not considering the vertices lying on the boundary Γ, whose amount, however, is negligible with respect to the total number of vertices in the triangulation, as the later becomes finer.

Now, it is well known that each tensor in $[\mathbb{RT}_0(T)^{\mathrm{t}}]^3$ is uniquely determined by its normal components on the 4 faces of T. Hence, since each interior face of $\mathcal{T}_h$ belongs to 2 tetrahedrons of $\mathcal{T}_h$, we find that the degrees of freedom defining $H_{0,h}^{\sigma}$ are given, approximately, by:

$$\left(\frac{3 \times 4}{2}\right) \times m = 6 \times m.$$

Finally, it is straightforward to see that the degrees of freedom defining H_h^{γ} are given by $3 \times m$, and hence the number of unknowns of the augmented scheme (4.1) with $\mathbf{H}_{0,h}$ given by (4.7), does in fact behave approximately as $9.5 \times m$.

Following a similar analysis one can easily show that the degrees of freedom defining the classical *PEERS* in 3D (see, e.g., Definition 3.1 in [6]) behaves approximately as $12.5 \times m$. Certainly, one could use static condensation to eliminate the 3 local degrees of freedom associated with the bubble function of each tetrahedron. However, this reduction by a factor of 3 also holds in the augmented formulation when the subspace $\mathbf{H}_{0,h}$ (cf. (4.7)) is employed since then one can use static condensation to eliminate the rotation $\boldsymbol{\gamma}_h$.

On the other hand, in what follows we compare and relate our augmented scheme with the mixed finite element methods that have emerged recently from the finite element exterior calculus (see, e.g. [14–16]). We begin by mentioning that the finite element subspaces of the Arnold–Falk–Winther (AFW) family described in [15] are all stable for the original dual-mixed formulation with weakly imposed symmetry (cf. (2.4) and (2.11)). In particular the lowest order member of this family is defined by

$$\mathbf{X}_h := X_h^{\sigma} \times X_h^{\mathbf{u}} \times X_h^{\gamma},$$

where

$$X_h^{\sigma} := \{\boldsymbol{\tau}_h \in H(\mathbf{div}; \Omega) : \boldsymbol{\tau}_{h,i}|_T \in [\mathbb{P}_1(T)]^3 \ \forall i \in \{1, 2, 3\}, \ \forall T \in \mathcal{T}_h\}, \tag{4.8}$$

$$X_h^{\mathbf{u}} := \{\mathbf{v}_h \in [L^2(\Omega)]^3 : \quad \mathbf{v}_h|_T \in [\mathbb{P}_0(T)]^3 \,\forall\, T \in \mathcal{T}_h\}, \tag{4.9}$$

and

$$X_h^{\boldsymbol{\gamma}} := \{\boldsymbol{\eta}_h \in [L^2(\Omega)]_{\mathrm{asym}}^{3\times 3} : \quad \boldsymbol{\eta}_h|_T \in [\mathbb{P}_0(T)]^{3\times 3} \,\forall\, T \in \mathcal{T}_h\}. \tag{4.10}$$

In other words, $X_h^{\boldsymbol{\sigma}}$ may be interpreted as the product of three copies of the Nédélec subspace of the second kind of degree 1 (cf. [17]), and $X_h^{\mathbf{u}}$ and $X_h^{\boldsymbol{\gamma}}$ are the usual subspaces of $[L^2(\Omega)]^3$ and $[L^2(\Omega)]_{\mathrm{asym}}^{3\times 3}$, respectively, of piecewise constant polynomials. Note that $H_h^{\boldsymbol{\sigma}}$ (cf. (4.3)) is strictly contained in $X_h^{\boldsymbol{\sigma}}$, and $H_h^{\boldsymbol{\gamma}}$ (cf. (4.6)) coincides with $X_h^{\boldsymbol{\gamma}}$. Also, $X_h^{\mathbf{u}}$, being given by piecewise constants, is clearly simpler than $H_h^{\mathbf{u}}$, but the latter yields continuous approximations of the displacements, which, from a physical point of view, may be considered as an advantage. Now, with respect to the number of unknowns involved, we know from [15] (see also [16]) that $X_h^{\boldsymbol{\sigma}}$ has 36 local degrees of freedom (9 per face of each tetrahedron), and hence the number of degrees of freedom defining $X_h^{\boldsymbol{\sigma}}$ is given, approximately, by

$$\left(\frac{36}{2}\right) \times m = 18 \times m.$$

This number reduces to $12 \times m$ when the corresponding AFW reduced element (see [15,16]) is employed. In this way, since $X_h^{\mathbf{u}}$ and $X_h^{\boldsymbol{\gamma}}$ are determined by $3 \times m$ degrees of freedom each, we deduce that the number of unknowns of the mixed finite element scheme arising from the formulation (2.11) and the finite element subspace $\mathbf{X}_h$, behaves approximately as $18 \times m$ (almost twice $9.5 \times m$, the number of unknowns of the augmented scheme (4.1) with (4.7)). Still, if we do not count the unknowns that can be eliminated by static condensation in each case, then we would have to compare $12 \times m$ with $6.5 \times m$, respectively.

We now recall the approximation properties of $H_{0,h}^{\boldsymbol{\sigma}}$, $H_h^{\mathbf{u}}$, and $H_h^{\boldsymbol{\gamma}}$ (see, e.g., [8,18]):

($\mathrm{AP}_{h,0}^{\boldsymbol{\sigma}}$) For each $\boldsymbol{\tau} \in [H^1(\Omega)]^{3\times 3} \cap H_0$ with $\mathbf{div}(\boldsymbol{\tau}) \in [H^1(\Omega)]^3$ there exists $\boldsymbol{\tau}_h \in H_{0,h}^{\boldsymbol{\sigma}}$ such that

$$\|\boldsymbol{\tau} - \boldsymbol{\tau}_h\|_{H(\mathbf{div};\,\Omega)} \leq C\,h\,\left\{\|\boldsymbol{\tau}\|_{[H^1(\Omega)]^{3\times 3}} + \|\mathbf{div}(\boldsymbol{\tau})\|_{[H^1(\Omega)]^3}\right\}.$$

($\mathrm{AP}_h^{\mathbf{u}}$) For each $\mathbf{v} \in [H^2(\Omega)]^3$ there exists $\mathbf{v}_h \in H_h^{\mathbf{u}}$ such that

$$\|\mathbf{v} - \mathbf{v}_h\|_{[H^1(\Omega)]^3} \leq C\,h\,\|\mathbf{v}\|_{[H^2(\Omega)]^3}.$$

($\mathrm{AP}_h^{\boldsymbol{\gamma}}$) For each $\boldsymbol{\eta} \in [H^1(\Omega)]_{\mathrm{asym}}^{3\times 3}$ there exists $\boldsymbol{\eta}_h \in H_h^{\boldsymbol{\gamma}}$ such that

$$\|\boldsymbol{\eta} - \boldsymbol{\eta}_h\|_{[L^2(\Omega)]^{3\times 3}} \leq C\,h\,\|\boldsymbol{\eta}\|_{[H^1(\Omega)]^{3\times 3}}.$$

Then, as a consequence of the Cea estimate (4.2), the above approximation properties, and the interpolation theorems in the corresponding function spaces, we can establish the 3D analogue of Theorem 4.2 in [5] as follows.

Theorem 4.1. *Let* $(\boldsymbol{\sigma}, \mathbf{u}, \boldsymbol{\gamma}) \in \mathbf{H}_0$ *and* $(\boldsymbol{\sigma}_h, \mathbf{u}_h, \boldsymbol{\gamma}_h) \in \mathbf{H}_{0,h} := H_{0,h}^{\boldsymbol{\sigma}} \times H_h^{\mathbf{u}} \times H_h^{\boldsymbol{\gamma}}$ *be the unique solutions of the continuous and discrete augmented mixed formulations (3.1) and (4.1), respectively. Assume that* $\boldsymbol{\sigma} \in [H^s(\Omega)]^{3\times 3}$, $\mathbf{div}(\boldsymbol{\sigma}) \in [H^s(\Omega)]^3$, $\mathbf{u} \in [H^{s+1}(\Omega)]^3$, *and* $\boldsymbol{\gamma} \in [H^s(\Omega)]^{3\times 3}$, *for some* $s \in (0, 1]$. *Then there exists* $C > 0$, *independent of* λ *and* h, *such that*

$$\|(\boldsymbol{\sigma}, \mathbf{u}, \boldsymbol{\gamma}) - (\boldsymbol{\sigma}_h, \mathbf{u}_h, \boldsymbol{\gamma}_h)\|_{\mathbf{H}_0} \leq C\,h^s\,\left\{\|\boldsymbol{\sigma}\|_{[H^s(\Omega)]^{3\times 3}} + \|\mathbf{div}(\boldsymbol{\sigma})\|_{[H^s(\Omega)]^3} + \|\mathbf{u}\|_{[H^{s+1}(\Omega)]^3} + \|\boldsymbol{\gamma}\|_{[H^s(\Omega)]^{3\times 3}}\right\}.$$

Finally, in order to deal with the mean value condition required by the traces of the elements in $H_{0,h}^{\boldsymbol{\sigma}}$, we proceed as in [1, 5] and replace (4.1) by the modified discrete scheme: Find $(\boldsymbol{\sigma}_h, \mathbf{u}_h, \boldsymbol{\gamma}_h, \rho_h) \in H_h^{\boldsymbol{\sigma}} \times H_h^{\mathbf{u}} \times H_h^{\boldsymbol{\gamma}} \times \mathbb{R}$ such that

$$\begin{aligned} A((\boldsymbol{\sigma}_h, \mathbf{u}_h, \boldsymbol{\gamma}_h), (\boldsymbol{\tau}_h, \mathbf{v}_h, \boldsymbol{\eta}_h)) + \rho_h \int_\Omega \mathrm{tr}(\boldsymbol{\tau}_h) &= F(\boldsymbol{\tau}_h, \mathbf{v}_h, \boldsymbol{\eta}_h), \\ \chi_h \int_\Omega \mathrm{tr}(\boldsymbol{\sigma}_h) &= 0, \end{aligned} \tag{4.11}$$

for all $(\boldsymbol{\tau}_h, \mathbf{v}_h, \boldsymbol{\eta}_h, \chi_h) \in H_h^{\boldsymbol{\sigma}} \times H_h^{\mathbf{u}} \times H_h^{\boldsymbol{\gamma}} \times \mathbb{R}$. The equivalence between (4.1) and (4.11) can be established analogously as Theorem 4.3 in [5]. We omit further details.

5. The case of homogeneous Dirichlet boundary conditions

In this section we assume that the Dirichlet datum $\mathbf{g} = \mathbf{0}$. It follows from our analysis in Section 2 that the original stress tensor $\boldsymbol{\sigma}$ belongs to H_0. In addition, since the displacement $\mathbf{u}$ lives now in $[H_0^1(\Omega)]^3$, we do not require the modified Korn inequality (3.5). Instead of it, we use the first Korn inequality (see, e.g. Theorem 10.1 in [4]), which establishes that

$$\|\mathbf{e}(\mathbf{v})\|_{[L^2(\Omega)]^{3\times 3}}^2 \geq \frac{1}{2}\,|\mathbf{v}|_{[H^1(\Omega)]^3}^2 \quad \forall\, v \in [H_0^1(\Omega)]^3. \tag{5.1}$$

Consequently, there is no need of introducing the boundary consistent term, and hence our augmented dual-mixed variational formulation reduces to: Find $(\boldsymbol{\sigma}, \mathbf{u}, \boldsymbol{\gamma}) \in \tilde{\mathbf{H}}_0 := H_0 \times [H_0^1(\Omega)]^3 \times [L^2(\Omega)]_{\text{asym}}^{3\times 3}$ such that

$$\tilde{A}((\boldsymbol{\sigma}, \mathbf{u}, \boldsymbol{\gamma}), (\boldsymbol{\tau}, \mathbf{v}, \boldsymbol{\eta})) = \tilde{F}(\boldsymbol{\tau}, \mathbf{v}, \boldsymbol{\eta}) \quad \forall (\boldsymbol{\tau}, \mathbf{v}, \boldsymbol{\eta}) \in \tilde{\mathbf{H}}_0, \tag{5.2}$$

where the bilinear form $\tilde{A} : \tilde{\mathbf{H}}_0 \times \tilde{\mathbf{H}}_0 \to \mathbb{R}$ and the linear functional $\tilde{F} : \tilde{\mathbf{H}}_0 \to \mathbb{R}$ are defined by

$$\begin{aligned} \tilde{A}((\boldsymbol{\sigma}, \mathbf{u}, \boldsymbol{\gamma}), (\boldsymbol{\tau}, \mathbf{v}, \boldsymbol{\eta})) := &\int_\Omega \mathcal{C}^{-1}\boldsymbol{\sigma} : \boldsymbol{\tau} + \int_\Omega \mathbf{u} \cdot \mathbf{div}(\boldsymbol{\tau}) + \int_\Omega \boldsymbol{\gamma} : \boldsymbol{\tau} - \int_\Omega \mathbf{v} \cdot \mathbf{div}(\boldsymbol{\sigma}) - \int_\Omega \boldsymbol{\eta} : \boldsymbol{\sigma} \\ &+ \kappa_1 \int_\Omega \left(\mathbf{e}(\mathbf{u}) - \mathcal{C}^{-1}\boldsymbol{\sigma} \right) : \left(\mathbf{e}(\mathbf{v}) + \mathcal{C}^{-1}\boldsymbol{\tau} \right) + \kappa_2 \int_\Omega \mathbf{div}(\boldsymbol{\sigma}) \cdot \mathbf{div}(\boldsymbol{\tau}) \\ &+ \kappa_3 \int_\Omega \left(\boldsymbol{\gamma} - \frac{1}{2}(\nabla\mathbf{u} - (\nabla\mathbf{u})^{\mathrm{t}}) \right) : \left(\boldsymbol{\eta} + \frac{1}{2}(\nabla\mathbf{v} - (\nabla\mathbf{v})^{\mathrm{t}}) \right), \end{aligned} \tag{5.3}$$

and

$$\tilde{F}(\boldsymbol{\tau}, \mathbf{v}, \boldsymbol{\eta}) := \int_\Omega \mathbf{f} \cdot (\mathbf{v} - \kappa_2 \, \mathbf{div}(\boldsymbol{\tau})). \tag{5.4}$$

In this way, following the same procedure of Section 3, we can replace our previous Theorem 3.1 by the following result, which is the 3D analogue of Theorem 3.1 in [1]. Note, as announced in Section 1, that all the stabilization parameters are determined explicitly by the Lamé constant μ.

Theorem 5.1. *Assume that $(\kappa_1, \kappa_2, \kappa_3)$ is independent of λ and such that $0 < \kappa_1 < 2\mu$, $0 < \kappa_2$, and $0 < \kappa_3 < \kappa_1$. Then, there exist positive constants M, α, independent of λ, such that*

$$|\tilde{A}((\boldsymbol{\sigma}, \mathbf{u}, \boldsymbol{\gamma}), (\boldsymbol{\tau}, \mathbf{v}, \boldsymbol{\eta}))| \leq M \, \|(\boldsymbol{\sigma}, \mathbf{u}, \boldsymbol{\gamma})\|_{\tilde{\mathbf{H}}_0} \, \|(\boldsymbol{\tau}, \mathbf{v}, \boldsymbol{\eta})\|_{\tilde{\mathbf{H}}_0},$$

and

$$\tilde{A}((\boldsymbol{\tau}, \mathbf{v}, \boldsymbol{\eta}), (\boldsymbol{\tau}, \mathbf{v}, \boldsymbol{\eta})) \geq \alpha \|(\boldsymbol{\tau}, \mathbf{v}, \boldsymbol{\eta})\|_{\tilde{\mathbf{H}}_0}^2$$

for all $(\boldsymbol{\sigma}, \mathbf{u}, \boldsymbol{\gamma})$, $(\boldsymbol{\tau}, \mathbf{v}, \boldsymbol{\eta}) \in \tilde{\mathbf{H}}_0$, where

$$\|(\boldsymbol{\tau}, \mathbf{v}, \boldsymbol{\eta})\|_{\tilde{\mathbf{H}}_0} := \left\{ \|\boldsymbol{\tau}\|_{H(\mathbf{div};\,\Omega)}^2 + |\mathbf{v}|_{[H^1(\Omega)]^3}^2 + \|\boldsymbol{\eta}\|_{[L^2(\Omega)]^{3\times 3}}^2 \right\}^{1/2} \quad \forall (\boldsymbol{\tau}, \mathbf{v}, \boldsymbol{\eta}) \in \tilde{\mathbf{H}}_0.$$

In particular, taking $\kappa_1 = C_1 \mu$, $\kappa_2 = \frac{1}{\mu}\left(1 - \frac{\kappa_1}{2\mu}\right)$, and $\kappa_3 = C_3 \kappa_1$, with any $C_1 \in \,]0, 2[$ and any $C_3 \in \,]0, 1[$, yields M and α depending only on μ, $\frac{1}{\mu}$, and c_1.

Next, given an arbitrary finite element subspace $\tilde{\mathbf{H}}_{0,h} \subseteq \tilde{\mathbf{H}}_0$, the Galerkin scheme associated with (5.2) reads: Find $(\boldsymbol{\sigma}_h, \mathbf{u}_h, \boldsymbol{\gamma}_h) \in \tilde{\mathbf{H}}_{0,h}$ such that

$$\tilde{A}((\boldsymbol{\sigma}_h, \mathbf{u}_h, \boldsymbol{\gamma}_h), (\boldsymbol{\tau}_h, \mathbf{v}_h, \boldsymbol{\eta}_h)) = \tilde{F}(\boldsymbol{\tau}_h, \mathbf{v}_h, \boldsymbol{\eta}_h) \quad \forall (\boldsymbol{\tau}_h, \mathbf{v}_h, \boldsymbol{\eta}_h) \in \tilde{\mathbf{H}}_{0,h}. \tag{5.5}$$

In particular, we consider

$$\tilde{\mathbf{H}}_{0,h} := H_{0,h}^{\boldsymbol{\sigma}} \times H_{0,h}^{\mathbf{u}} \times H_h^{\boldsymbol{\gamma}}, \tag{5.6}$$

where $H_{0,h}^{\boldsymbol{\sigma}}$ and $H_h^{\boldsymbol{\gamma}}$ are defined by (4.4) and (4.6), respectively, and

$$H_{0,h}^{\mathbf{u}} := \{\mathbf{v}_h \in H_h^{\mathbf{u}} : \quad \mathbf{v}_h = \mathbf{0} \quad \text{on } \Gamma\}. \tag{5.7}$$

The rest of the analysis, including the well-posedness of (5.2) and (5.5), the corresponding a priori error estimates, and the rates of convergences, follows exactly as in Sections 3 and 4. We omit further details.

6. Numerical results

In this section we present several examples illustrating the performance of the augmented mixed finite element schemes (4.1) and (5.5), with $\mathbf{H}_{0,h}$ and $\tilde{\mathbf{H}}_{0,h}$ given by (4.7) and (5.6), respectively, on a finite sequence of uniform meshes of the domain Ω. In what follows, N stands for the total number of degrees of freedom of the discrete schemes, which behaves approximately as $9.5 \times m$, where m is the number of tetrahedrons of each triangulation Also, the individual and total errors are denoted by

$$e(\boldsymbol{\sigma}) := \|\boldsymbol{\sigma} - \boldsymbol{\sigma}_h\|_{H(\mathbf{div};\,\Omega)}, \qquad e_0(\boldsymbol{\sigma}) := \|\boldsymbol{\sigma} - \boldsymbol{\sigma}_h\|_{[L^2(\Omega)]^{3\times 3}}, \qquad e(\mathbf{u}) := \|\mathbf{u} - \mathbf{u}_h\|_{[H^1(\Omega)]^3},$$

$$e(\boldsymbol{\gamma}) := \|\boldsymbol{\gamma} - \boldsymbol{\gamma}_h\|_{[L^2(\Omega)]^{3\times 3}}, \quad \text{and} \quad e(\boldsymbol{\sigma}, \mathbf{u}, \boldsymbol{\gamma}) := \left\{ [e(\boldsymbol{\sigma})]^2 + [e(\mathbf{u})]^2 + [e(\boldsymbol{\gamma})]^2 \right\}^{1/2}.$$

In addition, we let $r(\boldsymbol{\sigma}), r_0(\boldsymbol{\sigma}), r(\mathbf{u}), r(\boldsymbol{\gamma})$ and $r(\boldsymbol{\sigma}, \mathbf{u}, \boldsymbol{\gamma})$ be the corresponding experimental rates of convergence, which are given by

$$r(\boldsymbol{\sigma}) := \frac{\log(e(\boldsymbol{\sigma})/e'(\boldsymbol{\sigma}))}{\log(h/h')}, \qquad r_0(\boldsymbol{\sigma}) := \frac{\log(e_0(\boldsymbol{\sigma})/e'_0(\boldsymbol{\sigma}))}{\log(h/h')}, \qquad r(\mathbf{u}) := \frac{\log(e(\mathbf{u})/e'(\mathbf{u}))}{\log(h/h')},$$

$$r(\boldsymbol{\gamma}) := \frac{\log(e(\boldsymbol{\gamma})/e'(\boldsymbol{\gamma}))}{\log(h/h')}, \quad \text{and} \quad r(\boldsymbol{\sigma}, \mathbf{u}, \boldsymbol{\gamma}) := \frac{\log(e(\boldsymbol{\sigma}, \mathbf{u}, \boldsymbol{\gamma})/e'(\boldsymbol{\sigma}, \mathbf{u}, \boldsymbol{\gamma}))}{\log(h/h')},$$

where h and h' denote two consecutive meshsizes with corresponding errors e and e'.

Next, we recall that given the Young modulus E and the Poisson ratio ν of an isotropic linear elastic solid, the corresponding Lamé parameters are defined as

$$\mu := \frac{E}{2(1+\nu)} \quad \text{and} \quad \lambda := \frac{E\nu}{(1+\nu)(1-2\nu)}.$$

In the examples we fix $E = 1$ and take $\nu \in \{0.3000, 0.4900, 0.4999\}$, which gives the following values of μ and λ:

ν	μ	λ
0.3000	0.3846	0.5769
0.4900	0.3356	16.4430
0.4999	0.3333	1666.4444

Certainly, the cases $\nu = 0.4900$ and $\nu = 0.4999$ correspond to materials showing nearly incompressible behaviours.

The numerical results given below were obtained in a *Pentium Xeon computer with dual processors*, using MATLAB codes. The Galerkin schemes (4.1) and (5.5) are implemented in these codes following Section 4.3 in [1], and they are solved by a direct method. The individual errors are computed on each tetrahedron using a Gaussian quadrature rule.

6.1. Non-homogeneous Dirichlet boundary conditions

In what follows we present three examples illustrating the performance of (4.1) with $\mathbf{H}_{0,h}$ given by (4.7). According to Theorem 3.1, we consider $\kappa_1 = C_1\mu$, $\kappa_2 = \frac{1}{\mu}\left(1 - \frac{\kappa_1}{2\mu}\right)$, $\kappa_3 = C_3\kappa_1$, and $\kappa_4 = \kappa_1 + \kappa_3$, with any $C_1 \in \,]0, 2[$ and $C_3 \in \,]0, \frac{\kappa_0}{1-\kappa_0}[$. In particular, we take $C_1 = 1$ and $C_3 \in \{\frac{1}{8}, \frac{1}{4}\}$, which yield, respectively,

$$(\kappa_1, \kappa_2, \kappa_3, \kappa_4) = \left(\mu, \frac{1}{2\mu}, \frac{\mu}{8}, \frac{9\mu}{8}\right) \quad \text{and} \quad (\kappa_1, \kappa_2, \kappa_3, \kappa_4) = \left(\mu, \frac{1}{2\mu}, \frac{\mu}{4}, \frac{5\mu}{4}\right). \tag{6.1}$$

Certainly, since κ_0 is unknown, we have assumed here that $\frac{1}{4} < \frac{\kappa_0}{1-\kappa_0}$. As we observe in the tables below, these choices of C_3 work fine. Otherwise, we would have to decrease this constant.

We take the domain Ω either as the unit cube $]0, 1[^3$ or the L-shaped domain

$$]-1/2, 1/2[\times]0, 1[\times]-1/2, 1/2[- \big\{]0, 1/2[\times]0, 1[\times]0, 1/2[\big\},$$

and choose the datum $\mathbf{f}$ so that the Poisson ratio ν and the exact solution $\mathbf{u} := (u_1, u_2, u_3)^{\mathrm{t}}$ of each example are given as follows:

EXAMPLE	Ω	ν	$\mathbf{u}(x_1, x_2, x_3)$
1	Unit cube	0.4900	$(x_1^2 + 1)(x_2^2 + 1)(x_3^2 + 1)e^{x_1+x_2+x_3}\begin{pmatrix}1\\1\\1\end{pmatrix}$
2	L-shaped	0.4999	$\dfrac{A}{r^3}\begin{pmatrix}(x_1 - 0.25)^2\\(x_1 - 0.25)(x_2 - 0.5)\\(x_1 - 0.25)(x_3 - 0.25)\end{pmatrix} + \dfrac{B}{r}\begin{pmatrix}1\\0\\0\end{pmatrix}$
3	L-shaped	0.3000	$r^{5/3}\sin((2\theta - \pi)/3)\,e^{x_2}\begin{pmatrix}1\\1\\1\end{pmatrix}$

where $r = \sqrt{(x_1 - 0.25)^2 + (x_2 - 0.5)^2 + (x_3 - 0.25)^2}$, $A = \frac{1}{16\pi\mu(1-\nu)}$, and $B = \frac{(3-4\nu)}{16\pi\mu(1-\nu)}$ in Example 2, whereas $r = \sqrt{x_1^2 + x_3^2}$ and $\theta = \arctan\left(\frac{x_3}{x_1}\right)$ in Example 3. Note that the solution of Example 2 is the Kelvin fundamental solution at $\mathbf{x}_0 := (0.25, 0.5, 0.25)^{\mathrm{t}}$, which is a smooth function since $\mathbf{x}_0$ lies outside the domain. Also, we observe that the solution of Example 3 is singular at $x_1 = x_3 = 0$. In fact, because of the power of r, we find that $\mathbf{div}(\boldsymbol{\sigma})$ belongs to $[H^{2/3}(\Omega)]^3$, whence Theorem 4.1 yields an a priori rate of convergence of $O(h^{2/3})$.

The meshsizes h, the number of unknowns N, and the number of tetrahedrons m of the uniform meshes employed in the simulations are displayed in Table 6.1. We see here that the ratios N/m form a decreasing sequence approaching 9.5,

Table 6.1
Ratios between number of unknowns and number of elements for Examples 1, 2, and 3.

Mesh	Example 1				Examples 2 and 3			
	h	N	m	N/m	h	N	m	N/m
1	0.5000	585	48	12.188	0.5000	462	36	12.833
2	0.3333	1 812	162	11.185	0.2500	3 171	288	11.010
3	0.2500	4 119	384	10.727	0.1666	10 182	972	10.475
4	0.2000	7 848	750	10.464	0.1250	23 547	2 304	10.220
5	0.1667	13 341	1 296	10.294	0.1000	45 318	4 500	10.071
6	0.1428	20 940	2 058	10.175	0.0833	77 547	7 776	9.973
7	0.1250	30 987	3 072	10.087	0.0714	122 286	12 348	9.903
8	0.1111	43 824	4 374	10.019	0.0625	181 587	18 432	9.852
9	0.1000	59 793	6 000	9.966				
10	0.0909	79 236	7 986	9.921				
11	0.0833	102 495	10 368	9.886				
12	0.0769	129 912	13 182	9.856				

Table 6.2
Individual and total errors, and experimental rates of convergence of Example 1 with $(\kappa_1, \kappa_2, \kappa_3, \kappa_4) = \left(\mu, \frac{1}{2\mu}, \frac{\mu}{8}, \frac{9\mu}{8}\right)$ and $(\kappa_1, \kappa_2, \kappa_3, \kappa_4) = \left(\mu, \frac{1}{2\mu}, \frac{\mu}{4}, \frac{5\mu}{4}\right)$.

N	$e(\boldsymbol{\sigma})$	$r(\boldsymbol{\sigma})$	$e(\mathbf{u})$	$r(\mathbf{u})$	$e(\boldsymbol{\gamma})$	$r(\boldsymbol{\gamma})$	$e(\boldsymbol{\sigma}, \mathbf{u}, \boldsymbol{\gamma})$	$r(\boldsymbol{\sigma}, \mathbf{u}, \boldsymbol{\gamma})$
585	2.296E+03	–	5.164E+02	–	3.061E+02	–	2.373E+03	–
1 812	1.579E+03	0.924	3.723E+02	0.807	3.620E+02	–	1.662E+03	0.879
4 119	1.203E+03	0.945	3.048E+02	0.695	4.025E+02	–	1.305E+03	0.841
7 848	9.709E+02	0.961	2.566E+02	0.770	4.177E+02	–	1.088E+03	0.815
13 341	8.125E+02	0.976	2.191E+02	0.867	4.170E+02	0.010	9.392E+02	0.805
20 940	6.975E+02	0.990	1.891E+02	0.958	4.073E+02	0.152	8.295E+02	0.805
30 987	6.102E+02	1.001	1.646E+02	1.036	3.930E+02	0.266	7.443E+02	0.812
43 824	5.418E+02	1.010	1.446E+02	1.102	3.767E+02	0.359	6.755E+02	0.822
59 793	4.868E+02	1.016	1.280E+02	1.157	3.599E+02	0.435	6.188E+02	0.833
79 236	4.417E+02	1.020	1.141E+02	1.204	3.432E+02	0.497	5.709E+02	0.845
102 495	4.041E+02	1.023	1.024E+02	1.244	3.272E+02	0.549	5.299E+02	0.855
129 912	3.722E+02	1.025	9.245E+01	1.278	3.121E+02	0.593	4.945E+02	0.865
585	2.293E+03	–	5.169E+02	–	2.396E+02	–	2.362E+03	–
1 812	1.569E+03	0.935	3.657E+02	0.854	2.722E+02	–	1.634E+03	0.909
4 119	1.189E+03	0.965	2.886E+02	0.823	2.843E+02	–	1.256E+03	0.915
7 848	9.549E+02	0.983	2.355E+02	0.912	2.796E+02	0.075	1.022E+03	0.922
13 341	7.965E+02	0.995	1.965E+02	0.993	2.675E+02	0.244	8.628E+02	0.931
20 940	6.823E+02	1.003	1.669E+02	1.060	2.526E+02	0.370	7.465E+02	0.940
30 987	5.964E+02	1.009	1.438E+02	1.113	2.374E+02	0.466	6.578E+02	0.947
43 824	5.294E+02	1.012	1.255E+02	1.155	2.228E+02	0.540	5.879E+02	0.954
59 793	4.757E+02	1.014	1.107E+02	1.190	2.091E+02	0.599	5.313E+02	0.960
79 236	4.319E+02	1.015	9.859E+01	1.218	1.966E+02	0.647	4.847E+02	0.965
102 495	3.954E+02	1.015	8.850E+01	1.241	1.853E+02	0.685	4.455E+02	0.969
129 912	3.645E+02	1.015	8.000E+01	1.260	1.749E+02	0.718	4.121E+02	0.972

which is coherent with the behaviour derived in Section 4. Then, in Tables 6.2–6.4 we present the individual and total errors, and the experimental rates of convergence for Examples 1, 2, and 3. We observe that the order $O(h)$ provided by Theorem 4.1 (when $s = 1$) is attained asymptotically in Examples 1 and 2. However, we notice that the rate of convergence of $e(\boldsymbol{\gamma})$ approaches 1 more slowly than the rates of convergence of the other errors. In particular, this influences the global rate of convergence in Example 2, which approaches 1 very slowly, as well. Anyway, this behaviour improves when $(\kappa_1, \kappa_2, \kappa_3, \kappa_4) = \left(\mu, \frac{1}{2\mu}, \frac{\mu}{4}, \frac{5\mu}{4}\right)$. On the other hand, the global rate of convergence in Example 3, which is determined by the dominant error $e(\boldsymbol{\sigma})$, does not approach 1 and, because of the singularity of the solution, stays around 2/3, as predicted. Nevertheless, the partial error $e_0(\boldsymbol{\sigma})$ is not affected by the lack of regularity of the solution and it shows a rate of convergence of order $O(h)$. Certainly, the low rate of convergence of $e(\boldsymbol{\sigma})$ in this example motivates the future development of a posteriori error estimates and the corresponding adaptive algorithms, as done for the 2D case in [3]. Next, we realize that in Example 1 the rate of convergence of $e(\mathbf{u})$ is somewhat larger than 1, which, however, seems a special behaviour of this particular solution $\mathbf{u}$.

6.2. Homogeneous Dirichlet boundary conditions

We now present two examples illustrating the performance of (5.5) with $\tilde{\mathbf{H}}_{0,h}$ given by (5.6). The mean value condition required by the traces of the elements in $H_{0,h}^{\sigma}$ is also imposed here as in (4.11). According to Theorem 5.1, we consider

Table 6.3

Individual and total errors, and experimental rates of convergence of Example 2 with $(\kappa_1, \kappa_2, \kappa_3, \kappa_4) = \left(\mu, \frac{1}{2\mu}, \frac{\mu}{8}, \frac{9\mu}{8}\right)$ and $(\kappa_1, \kappa_2, \kappa_3, \kappa_4) = \left(\mu, \frac{1}{2\mu}, \frac{\mu}{4}, \frac{5\mu}{4}\right)$.

N	$e(\boldsymbol{\sigma})$	$r(\boldsymbol{\sigma})$	$e(\mathbf{u})$	$r(\mathbf{u})$	$e(\boldsymbol{\gamma})$	$r(\boldsymbol{\gamma})$	$e(\boldsymbol{\sigma}, \mathbf{u}, \boldsymbol{\gamma})$	$r(\boldsymbol{\sigma}, \mathbf{u}, \boldsymbol{\gamma})$
462	3.771E−01	–	4.772E−01	–	1.775E−01	–	6.335E−01	–
3 171	2.760E−01	0.450	3.588E−01	0.411	2.525E−01	–	5.183E−01	0.290
10 182	2.081E−01	0.696	2.790E−01	0.620	2.718E−01	–	4.416E−01	0.395
23 547	1.619E−01	0.874	2.247E−01	0.753	2.623E−01	0.123	3.814E−01	0.509
45 318	1.300E−01	0.981	1.866E−01	0.832	2.447E−01	0.312	3.341E−01	0.594
77 547	1.075E−01	1.044	1.588E−01	0.886	2.258E−01	0.440	2.962E−01	0.659
122 286	9.102E−02	1.080	1.377E−01	0.925	2.081E−01	0.532	2.656E−01	0.709
181 587	7.857E−02	1.102	1.212E−01	0.953	1.920E−01	0.601	2.403E−01	0.749
462	3.722E−01	–	4.827E−01	–	1.633E−01	–	6.310E−01	–
3 171	2.546E−01	0.548	3.579E−01	0.432	1.876E−01	–	4.775E−01	0.402
10 182	1.836E−01	0.806	2.768E−01	0.633	1.788E−01	0.118	3.772E−01	0.581
23 547	1.396E−01	0.952	2.221E−01	0.765	1.605E−01	0.374	3.076E−01	0.710
45 318	1.112E−01	1.019	1.840E−01	0.843	1.429E−01	0.523	2.582E−01	0.785
77 547	9.191E−02	1.047	1.564E−01	0.894	1.276E−01	0.620	2.218E−01	0.834
122 286	7.808E−02	1.057	1.355E−01	0.929	1.147E−01	0.690	1.940E−01	0.869
181 587	6.778E−02	1.059	1.193E−01	0.956	1.039E−01	0.742	1.721E−01	0.896

Table 6.4

Individual errors and experimental rates of convergence of Example 3 with $(\kappa_1, \kappa_2, \kappa_3, \kappa_4) = \left(\mu, \frac{1}{2\mu}, \frac{\mu}{8}, \frac{9\mu}{8}\right)$ and $(\kappa_1, \kappa_2, \kappa_3, \kappa_4) = \left(\mu, \frac{1}{2\mu}, \frac{\mu}{4}, \frac{5\mu}{4}\right)$.

N	$e(\boldsymbol{\sigma})$	$r(\boldsymbol{\sigma})$	$e(\mathbf{u})$	$r(\mathbf{u})$	$e(\boldsymbol{\gamma})$	$r(\boldsymbol{\gamma})$	$e_0(\boldsymbol{\sigma})$	$r_0(\boldsymbol{\sigma})$
462	1.278E−00	–	7.401E−01	–	5.046E−01	–	4.979E−01	–
3 171	8.601E−01	0.571	4.141E−01	0.838	3.560E−01	0.503	2.914E−01	0.773
10 182	6.693E−01	0.619	2.856E−01	0.916	2.993E−01	0.428	2.016E−01	0.909
23 547	5.578E−01	0.634	2.166E−01	0.961	2.563E−01	0.538	1.525E−01	0.969
45 318	4.835E−01	0.640	1.739E−01	0.985	2.220E−01	0.644	1.221E−01	0.996
77 547	4.300E−01	0.644	1.450E−01	0.998	1.946E−01	0.722	1.017E−01	1.007
122 286	3.893E−01	0.646	1.242E−01	1.005	1.727E−01	0.777	8.697E−02	1.012
181 587	3.570E−01	0.647	1.085E−01	1.009	1.548E−01	0.818	7.595E−02	1.014
462	1.275E−00	–	7.505E−01	–	3.576E−01	–	4.913E−01	–
3 171	8.565E−01	0.574	4.156E−01	0.853	2.437E−01	0.553	2.806E−01	0.808
10 182	6.667E−01	0.618	2.865E−01	0.917	1.894E−01	0.622	1.928E−01	0.925
23 547	5.560E−01	0.631	2.176E−01	0.957	1.540E−01	0.720	1.460E−01	0.967
45 318	4.823E−01	0.637	1.749E−01	0.978	1.290E−01	0.792	1.172E−01	0.984
77 547	4.291E−01	0.641	1.460E−01	0.990	1.107E−01	0.840	9.782E−02	0.992
122 286	3.886E−01	0.644	1.252E−01	0.997	9.675E−02	0.874	8.390E−02	0.996
181 587	3.565E−01	0.646	1.095E−01	1.002	8.581E−02	0.899	7.343E−02	0.998

Table 6.5

Ratio between number of unknowns and number of elements for Examples 4 and 5.

MESH	h	N	m	N/m
1	0.5000	507	48	10.562
2	0.3333	1 644	162	10.148
3	0.2500	3 825	384	9.960
4	0.2000	7 392	750	9.856
5	0.1667	12 687	1 296	9.789
6	0.1428	20 052	2 058	9.743
7	0.1250	29 829	3 072	9.709
8	0.1111	42 360	4 374	9.684
9	0.1000	57 987	6 000	9.664
10	0.0909	77 052	7 986	9.648
11	0.0833	99 897	10 368	9.635
12	0.0769	126 864	13 182	9.624

$\kappa_1 = C_1 \mu$, $\kappa_2 = \frac{1}{\mu}\left(1 - \frac{\kappa_1}{2\mu}\right)$ and $\kappa_3 = C_3 \kappa_1$, with any $C_1 \in (0, 2)$ and $C_3 \in (0, 1)$. In particular, we take $(C_1, C_3) = (1, \frac{1}{2})$ and $(C_1, C_3) = (\frac{3}{2}, \frac{2}{3})$, which yield, respectively,

$$(\kappa_1, \kappa_2, \kappa_3) = \left(\mu, \frac{1}{2\mu}, \frac{\mu}{2}\right) \quad \text{and} \quad (\kappa_1, \kappa_2, \kappa_3) = \left(\frac{3\mu}{2}, \frac{1}{4\mu}, \mu\right). \tag{6.2}$$

Table 6.6
Individual and total errors, and experimental rates of convergence of Example 4 with $(\kappa_1, \kappa_2, \kappa_3) = (\mu, \frac{1}{2\mu}, \frac{\mu}{2})$ and $(\kappa_1, \kappa_2, \kappa_3) = (\frac{3\mu}{2}, \frac{1}{4\mu}, \mu)$.

N	$e(\sigma)$	$r(\sigma)$	$e(\mathbf{u})$	$r(\mathbf{u})$	$e(\gamma)$	$r(\gamma)$	$e(\sigma, \mathbf{u}, \gamma)$	$r(\sigma, \mathbf{u}, \gamma)$
507	6.112E−01	–	4.609E−02	–	4.686E−02	–	6.148E−01	–
1 644	5.337E−01	0.334	6.288E−02	–	3.337E−02	0.836	5.384E−01	0.327
3 825	4.389E−01	0.679	4.619E−02	1.072	3.306E−02	0.032	4.426E−01	0.681
7 392	3.687E−01	0.781	3.405E−02	1.366	3.213E−02	0.127	3.717E−01	0.782
12 687	3.161E−01	0.843	2.581E−02	1.519	3.057E−02	0.272	3.186E−01	0.844
20 052	2.758E−01	0.884	2.017E−02	1.598	2.876E−02	0.395	2.780E−01	0.884
29 829	2.442E−01	0.911	1.618E−02	1.650	2.693E−02	0.494	2.462E−01	0.910
42 360	2.188E−01	0.931	1.326E−02	1.689	2.517E−02	0.572	2.206E−01	0.929
57 987	1.981E−01	0.944	1.106E−02	1.723	2.354E−02	0.635	1.998E−01	0.943
77 052	1.808E−01	0.954	9.360E−03	1.752	2.205E−02	0.685	1.824E−01	0.953
99 897	1.663E−01	0.962	8.019E−03	1.777	2.070E−02	0.727	1.678E−01	0.960
126 864	1.539E−01	0.968	6.943E−03	1.799	1.947E−02	0.761	1.553E−01	0.966
507	6.112E−01	–	1.862E−02	–	2.355E−02	–	6.120E−01	–
1 644	5.337E−01	0.334	2.695E−02	–	1.774E−02	–	5.346E−01	0.333
3 825	4.387E−01	0.680	2.130E−02	0.818	1.792E−02	–	4.396E−01	0.680
7 392	3.685E−01	0.782	1.617E−02	1.234	1.735E−02	0.146	3.692E−01	0.782
12 687	3.159E−01	0.844	1.242E−02	1.443	1.637E−02	0.316	3.165E−01	0.844
20 052	2.756E−01	0.885	9.779E−03	1.555	1.528E−02	0.448	2.762E−01	0.884
29 829	2.440E−01	0.911	7.868E−03	1.628	1.420E−02	0.549	2.445E−01	0.911
42 360	2.186E−01	0.930	6.452E−03	1.683	1.318E−02	0.627	2.191E−01	0.930
57 987	1.979E−01	0.944	5.379E−03	1.727	1.226E−02	0.688	1.984E−01	0.944
77 052	1.807E−01	0.954	4.547E−03	1.762	1.143E−02	0.736	1.811E−01	0.953
99 897	1.662E−01	0.961	3.890E−03	1.792	1.068E−02	0.774	1.666E−01	0.961
126 864	1.538E−01	0.967	3.364E−03	1.816	1.002E−02	0.805	1.542E−01	0.967

Table 6.7
Individual and total errors, and experimental rates of convergence of Example 5 with $(\kappa_1, \kappa_2, \kappa_3) = (\mu, \frac{1}{2\mu}, \frac{\mu}{2})$ and $(\kappa_1, \kappa_2, \kappa_3) = (\frac{3\mu}{2}, \frac{1}{4\mu}, \mu)$.

N	$e(\sigma)$	$r(\sigma)$	$e(\mathbf{u})$	$r(\mathbf{u})$	$e(\gamma)$	$r(\gamma)$	$e(\sigma, \mathbf{u}, \gamma)$	$r(\sigma, \mathbf{u}, \gamma)$
507	8.757E+01	–	1.446E+01	–	6.759E+00	–	8.901E+01	–
1 644	6.067E+01	0.904	8.706E+00	1.252	6.183E+00	0.219	6.161E+01	0.907
3 825	4.620E+01	0.947	5.803E+00	1.410	5.850E+00	0.192	4.693E+01	0.945
7 392	3.723E+01	0.967	4.203E+00	1.445	5.478E+00	0.294	3.787E+01	0.961
12 687	3.115E+01	0.978	3.225E+00	1.453	5.095E+00	0.397	3.173E+01	0.970
20 052	2.676E+01	0.985	2.573E+00	1.463	4.727E+00	0.486	2.729E+01	0.976
29 829	2.344E+01	0.990	2.112E+00	1.477	4.386E+00	0.559	2.394E+01	0.981
42 360	2.085E+01	0.994	1.772E+00	1.491	4.077E+00	0.620	2.132E+01	0.984
57 987	1.877E+01	0.996	1.512E+00	1.504	3.799E+00	0.669	1.921E+01	0.987
77 052	1.707E+01	0.997	1.309E+00	1.513	3.550E+00	0.710	1.748E+01	0.989
99 897	1.565E+01	0.999	1.147E+00	1.518	3.327E+00	0.745	1.604E+01	0.991
126 864	1.444E+01	0.999	1.015E+00	1.520	3.128E+00	0.773	1.481E+01	0.992
507	8.758E+01	–	7.003E+00	–	3.793E+00	–	8.794E+01	–
1 644	6.061E+01	0.907	4.553E+00	1.061	3.461E+00	0.225	6.088E+01	0.906
3 825	4.612E+01	0.949	3.249E+00	1.172	3.249E+00	0.220	4.634E+01	0.948
7 392	3.714E+01	0.969	2.461E+00	1.244	3.012E+00	0.338	3.735E+01	0.967
12 687	3.107E+01	0.980	1.948E+00	1.282	2.775E+00	0.449	3.125E+01	0.977
20 052	2.668E+01	0.986	1.592E+00	1.309	2.553E+00	0.541	2.685E+01	0.983
29 829	2.338E+01	0.990	1.333E+00	1.327	2.352E+00	0.614	2.353E+01	0.988
42 360	2.080E+01	0.993	1.139E+00	1.338	2.173E+00	0.673	2.094E+01	0.990
57 987	1.873E+01	0.994	9.890E−01	1.341	2.014E+00	0.720	1.886E+01	0.992
77 052	1.703E+01	0.996	8.706E−01	1.338	1.873E+00	0.758	1.715E+01	0.994
99 897	1.561E+01	0.997	7.752E−01	1.332	1.749E+00	0.788	1.573E+01	0.995
126 864	1.441E+01	0.997	6.973E−01	1.323	1.639E+00	0.814	1.452E+01	0.996

We take Ω as the unit cube $]0, 1[^3$ and choose the datum $\mathbf{f}$ so that the Poisson ratio ν and the exact solution $\mathbf{u} := (u_1, u_2, u_3)^{\mathrm{t}}$ of each example are given as follows:

EXAMPLE	ν	$\mathbf{u}(x_1, x_2, x_3)$
4	0.4999	$x_1^3(1-x_1)^2 x_2^3(1-x_2)^2 x_3^3(1-x_3)^2 \begin{pmatrix} 1 \\ 1 \\ 1 \end{pmatrix}$
5	0.4900	$\sin(\pi x_1)\sin(\pi x_2)\sin(\pi x_3) \begin{pmatrix} 1 \\ 1 \\ 1 \end{pmatrix}$

The meshsizes, the number of unknowns N, and the number of tetrahedrons m of the uniform meshes employed in the simulations are displayed in Table 6.5. The ratios N/m also form a decreasing sequence approaching 9.5. Then, in Tables 6.6 and 6.7, we present the individual and total errors, and the experimental rates of convergence for Examples 4 and 5. The remarks here are similar to those indicated in the non-homogeneous case. In fact, the order $O(h)$ is also attained in both Examples, but, as before, the rate of convergence of $e(\boldsymbol{\gamma})$ approaches 1 more slowly than the other rates of convergence. In addition, the apparent superconvergence of $e(\mathbf{u})$ is also present in these examples.

We end this section by remarking that the absence of significant differences between the simulations obtained in each case with the two sets of parameters (cf. (6.1) and (6.2)), confirms the robustness of the augmented mixed finite element schemes proposed in this paper.

Appendix. The modified Korn inequality

In this appendix we prove the modified Korn inequality (3.5). We first introduce the space of rigid body motions in Ω, that is

$$\mathbb{RM}(\Omega) := \left\{ \mathbf{w} : \Omega \to \mathbb{R}^3 \ : \ \mathbf{w}(\mathbf{x}) = \vec{a} + \vec{b} \times \mathbf{x}, \quad \vec{a}, \vec{b} \in \mathbb{R}^3 \right\}.$$

Also, we let $\mathcal{P} : [H^1(\Omega)]^3 \to \mathbb{RM}(\Omega)$ be the orthogonal projector with respect to the usual norm in $[H^1(\Omega)]^3$. Then, the Korn inequality in the quotient space $[H^1(\Omega)]^3/\mathbb{RM}(\Omega)$ (see, e.g., Theorem 2.2 in [12]) yields the existence of $C > 0$ such that

$$\|\mathbf{v} - \mathcal{P}(\mathbf{v})\|_{[H^1(\Omega)]^3} \leq C \, \|\mathbf{e}(\mathbf{v})\|_{[L^2(\Omega)]^{3\times3}} \quad \forall \mathbf{v} \in [H^1(\Omega)]^3. \tag{A.1}$$

We now recall one of the three statements provided by the Peetre–Tartar lemma (see, e.g. Theorem 2.1 in Chapter I of [13]), which is applied below in the proof of Lemma A.2.

Lemma A.1. *Let* $(E_1, \|\cdot\|_1)$, $(E_2, \|\cdot\|_2)$, *and* $(E_3, \|\cdot\|_3)$ *be Banach spaces, and let* $A : E_1 \to E_2$ *and* $B : E_1 \to E_3$ *be bounded linear operators such that* B *is compact. Assume that there exists* $C > 0$ *such that*

$$\|v\|_1 \leq C \left\{ \|A(v)\|_2 + \|B(v)\|_3 \right\} \quad \forall v \in E_1. \tag{A.2}$$

Then the null space $N(A)$ *of* A *is finite dimensional,* A *is an isomorphism from* $E_1/N(A)$ *onto the range* $R(A)$ *of* A, *and* $R(A)$ *is a closed subspace of* E_2, *that is there exists* $C_1 > 0$ *such that*

$$\mathrm{dist}(v, N(A)) := \inf_{z \in N(A)} \|v - z\|_1 \leq C_1 \, \|A(v)\|_2 \quad \forall v \in E_1. \tag{A.3}$$

We are now in a position to prove the modified Korn inequality (3.5).

Lemma A.2. *There exists* $\kappa_0 > 0$ *such that*

$$\|\mathbf{e}(\mathbf{v})\|_{[L^2(\Omega)]^{3\times3}}^2 + \|\mathbf{v}\|_{[L^2(\Gamma)]^3}^2 \geq \kappa_0 \, \|\mathbf{v}\|_{[H^1(\Omega)]^3}^2 \quad \forall \mathbf{v} \in [H^1(\Omega)]^3. \tag{A.4}$$

Proof. In order to apply Lemma A.1 we let $E_1 := [H^1(\Omega)]^3$, $E_2 := [L^2(\Omega)]^{3\times3} \times [L^2(\Gamma)]^3$, $E_3 := \mathbb{RM}(\Omega)$, and define the bounded linear operators $A : E_1 \to E_2$ and $B : E_1 \to E_3$ as

$$A(\mathbf{v}) := (\mathbf{e}(\mathbf{v}), \mathbf{v}|_\Gamma) \quad \forall \mathbf{v} \in [H^1(\Omega)]^3 \quad \text{and} \quad B := \mathcal{P}.$$

It is clear that B is bounded and compact. Then, using triangle inequality and (A.1), we find that

$$\|\mathbf{v}\|_{[H^1(\Omega)]^3} \leq \|\mathbf{v} - \mathcal{P}(\mathbf{v})\|_{[H^1(\Omega)]^3} + \|\mathcal{P}(\mathbf{v})\|_{[H^1(\Omega)]^3} \leq C \left\{ \|\mathbf{e}(\mathbf{v})\|_{[L^2(\Omega)]^{3\times3}} + \|B(\mathbf{v})\|_{[H^1(\Omega)]^3} \right\},$$

which yields (A.2). In this way, noting that $N(A) = \{0\}$, the inequality (A.3) yields (A.4). □

References

[1] G.N. Gatica, Analysis of a new augmented mixed finite element method for linear elasticity allowing $\mathbb{RT}_0 - \mathbb{P}_1 - \mathbb{P}_0$ approximations, M2AN Mathematical Modelling and Numerical Analysis 40 (1) (2006) 1–28.
[2] D.N. Arnold, F. Brezzi, J. Douglas, PEERS: A new mixed finite element method for plane elasticity, Japan Journal of Applied Mathematics 1 (1984) 347–367.
[3] T.P. Barrios, G.N. Gatica, M. González, N. Heuer, A residual based a posteriori error estimator for an augmented mixed finite element method in linear elasticity, M2AN Mathematical Modelling and Numerical Analysis 40 (5) (2006) 843–869.
[4] W. McLean, Strongly Elliptic Systems and Boundary Integral Equations, Cambridge University Press, 2000.
[5] G.N. Gatica, An augmented mixed finite element method for linear elasticity with non homogeneous Dirichlet conditions, Electronic Transactions on Numerical Analysis 26 (2007) 421–438.

 [6] M. Lonsing, R. Verfürth, On the stability of BDMS and PEERS elements, Numerische Mathematik 99 (1) (2004) 131–140.
 [7] R. Stenberg, A family of mixed finite elements for the elasticity problem, Numerische Mathematik 53 (5) (1988) 513–538.
 [8] F. Brezzi, M. Fortin, Mixed and Hybrid Finite Element Methods, Springer Verlag, 1991.
 [9] D.N. Arnold, R.S. Falk, Well-posedness of the fundamental boundary problems for constrained anisotropic elastic materials, Archive for Rational Mechanics and Analysis 98 (1987) 143–190.
[10] D.N. Arnold, J. Douglas, Ch.P. Gupta, A family of higher order mixed finite element methods for plane elasticity, Numerische Mathematik 45 (1984) 1–22.
[11] S.C. Brenner, L.R. Scott, The Mathematical Theory of Finite Element Methods, Springer-Verlag New York, 1994.
[12] P.G. Ciarlet, P. Ciarlet, Another approach to linearized elasticity and a new proof of Korn's inequality, Mathematical Models and Methods in Applied Analysis 15 (2) (2005) 259–271.
[13] V. Girault, P.-A. Raviart, Finite Element Methods for Navier–Stokes Equations: Theory and Algorithms, in: Springer Series in Computational Mathematics, vol. 5, 1986.
[14] D.N. Arnold, R.S. Falk, R. Winther, Finite element exterior calculus, homological techniques, and applications, Acta Numerica 15 (2006) 1–155.
[15] D.N. Arnold, R.S. Falk, R. Winther, Mixed finite element methods for linear elasticity with weakly imposed symmetry, Mathematics of Computation 76 (260) (2007) 1699–1723.
[16] R.S. Falk, Finite element methods for linear elasticity, in: D. Boffi, L. Gastaldi (Eds.), Mixed Finite Elements, Compatibility Conditions and Applications, Springer, 2008.
[17] J.-C. Nédélec, A new family of mixed finite elements in $\mathbb{R}^3$, Numerische Mathematik 50 (1) (1986) 57–81.
[18] P.G. Ciarlet, The Finite Element Method for Elliptic Problems, North-Holland, 1978.